Journal of Wind Engineering & Industrial Aerodynamics 220 (2022) 104806

Contents lists available at ScienceDirect

Journal of Wind Engineering & Industrial Aerodynamics

journal homepage: www.elsevier.com/locate/jweia

Bridge buffeting by skew winds: A revised theory

Bernardo Morais da Costa [a,b,*], Jungao Wang [a,b], Jasna Bogunović Jakobsen [a], Ole Andre Øiseth [c], Jónas Þór Snæbjörnsson [a,d]

[a] Department of Mechanical and Structural Engineering and Materials Science, University of Stavanger, Kristine Bonnevies Vei 22, 4021, Stavanger, Norway
[b] Norwegian Public Roads Administration, Bergelandsgata 30, 4012, Stavanger, Norway
[c] Department of Structural Engineering, Norwegian University of Science and Technology, Richard Birkelands Vei 1A, 7491, Trondheim, Norway
[d] Department of Engineering, Reykjavik University, Menntavegur 1, 102, Reykjavík, Iceland

ARTICLE INFO

Keywords:
Skew wind
Yaw angle
Buffeting theory
Bridge aerodynamics
Quasi-steady motion-dependent forces
Curved bridge
Floating bridge
Cosine rule

ABSTRACT

An improved bridge buffeting theory is established with an emphasis on skew wind directions, for both turbulence- and motion-dependent forces. It provides simplifications and generalizations of previously established methods. The formulation starts with a preferred 3D approach, which is suitable when aerodynamic coefficients for different yaw and inclination angles are readily available. The 3D approach includes a new convenient choice of coordinate systems and an intuitive derivation of transformation matrices, supporting clear and compact wind load expressions as well as a more accurate formulation of the quasi-steady motion-dependent forces. When the aerodynamic coefficients have only been obtained for wind normal to the bridge girder, an alternative 2D approach is provided. The 2D approach, where only the normal projection of the wind is considered, is further expanded to include mean wind directions that are both yawed and inclined, axial forces in the longitudinal direction (1D) in an optional 2D + 1D format, and forces due to all in-plane and out-of-plane motions. All expressions are first presented in a compact non-linear format and then linearized through numerous multivariate Taylor series approximations. A general, more straightforward and more accurate framework is thus established for both time- and frequency-domain analyses of the buffeting response.

1. Introduction

Advances in economy and technology lead to increasingly innovative structures. In the field of bridge engineering, the planned bridge for Bjørnafjorden, in Norway, illustrated in Fig. 1a, is a notable example of a long, flexible and complex wind-exposed floating structure which drives the need for more accurate wind and aerodynamic prediction models.

Classical buffeting analyses of straight bridges, first introduced by (Davenport, 1961), deal with wind normal (perpendicular) to the bridge girder, which is often assumed to be the governing load case. Relevant aerodynamic parameters (e.g. aerodynamic coefficients and flutter derivatives) are usually obtained experimentally, in wind tunnel facilities, on a section of the bridge girder positioned perpendicularly to the mean wind direction.

When skew winds are considered, i.e. winds whose mean direction is not normal to the bridge longitudinal axis, the analyses are typically simplified to different extent. One common simplification is to decompose the wind into its normal and longitudinal components, discarding the latter one and proceeding with a 2D interaction problem in the normal plane. This is also referred to as the *cosine rule*, *cosine law* or *decomposition method*, which follow the so-called *independence principle* or *cross flow principle*.

This principle was first observed in circular wires under a subcritical flow regime (see e.g. (Jones, 1947) illustrating the original experimental results from (Relf and Powell, 1917)). Approximate laminar boundary layer equations for yawed infinite cylinders (Sears, 1948) and yawed swept back wings (Wild, 1949) further supported this principle. On the other hand, worse agreements were found for yawed cylinders near and above critical flow regimes (Bursnall and Loftin Jr, 1951), at high yaw angles ((Sumer, 2006) and (Ersdal and Faltinsen, 2006)), with respect to vortex induced vibrations (Van Atta, 1968), using CFD simulations to look at the flow structure (Wang et al., 2019), and in the recommended practice by (Veritas, 2010) which only supports this principle for yaw angles up to 45°.

The same principle was then also applied to bridges, with inconsis-

* Corresponding author. Department of Mechanical and Structural Engineering and Materials Science, University of Stavanger, Kristine Bonnevies vei 22, 4021, Stavanger, Norway.

E-mail addresses: bercos@vegvesen.no (B.M. da Costa), jungao.wang@vegvesen.no (J. Wang), jasna.b.jakobsen@uis.no (J.B. Jakobsen), ole.oiseth@ntnu.no (O.A. Øiseth), jonasthor@ru.is (J. Snæbjörnsson).

https://doi.org/10.1016/j.jweia.2021.104806
Received 24 December 2020; Received in revised form 13 September 2021; Accepted 8 October 2021
Available online 23 December 2021

Table of notations

Variables

β	Local mean yaw angle
$\tilde{\beta}$	Local instantaneous yaw angle (turbulence dependent)
$\tilde{\tilde{\beta}}$	Local instantaneous relative yaw angle (turbulence and motion dependent)
β_G	Global mean yaw angle
γ	A generic angle
$\Delta, \dot{\Delta}, \ddot{\Delta}$	Vectors of displacements, velocities, accelerations (for each element)
$\Delta^G, \dot{\Delta}^G, \ddot{\Delta}^G$	Global vectors of displacements, velocities, accelerations (for all nodes)
$\widetilde{\Delta\beta}$, $\widetilde{\widetilde{\Delta\beta}}$	Change in β due to: turbulence ($\widetilde{\Delta\beta}$), turbulence and structural motions ($\widetilde{\widetilde{\Delta\beta}}$)
$\widetilde{\Delta\theta}$, $\widetilde{\widetilde{\Delta\theta}}$	Change in θ due to: turbulence ($\widetilde{\Delta\theta}$), turbulence and structural motions ($\widetilde{\widetilde{\Delta\theta}}$)
$\widetilde{\Delta\theta}_{yz}$, $\widetilde{\widetilde{\Delta\theta}}_{\widetilde{yz}}$	Change in θ_{yz} due to: turbulence ($\widetilde{\Delta\theta}_{yz}$), turbulence and structural motions ($\widetilde{\widetilde{\Delta\theta}}_{\widetilde{yz}}$)
θ	Local mean inclination angle
$\tilde{\theta}$	Local instantaneous inclination angle (turbulence dependent)
$\tilde{\tilde{\theta}}$	Local instantaneous relative inclination angle (turbulence and motion dependent)
θ_{yz}, $\tilde{\theta}_{yz}$, $\tilde{\tilde{\theta}}_{yz}$	yz-plane projection counterparts of θ, $\tilde{\theta}$, $\tilde{\tilde{\theta}}$
θ_G	Global mean inclination angle
ρ	Air density
$\boldsymbol{\sigma}_\Delta$	Global vector of standard deviations of Δ (for all nodes)
$\boldsymbol{\Phi}$	Matrix of mode shapes
$\chi_{i,j}$	Cross-sectional admittance function, associated with C_i and turbulence component j
ω	Angular frequency (radians per second)
a_i, $\boldsymbol{a}_i$	a_i is the wind turbulence component in the i-axis (e.g. a_x). $\boldsymbol{a}_i$ is the wind turbulence vector in the i-system (e.g. $\boldsymbol{a}_{Gw} = [u, v, w]^T$)
$\tilde{\tilde{a}}_D$, $\tilde{\tilde{a}}_A$, $\tilde{\tilde{a}}_L$	Counterparts of $\tilde{\tilde{u}}$, $\tilde{\tilde{v}}$, $\tilde{\tilde{w}}$ in the Lnw-system
$\boldsymbol{A}_b$	Buffeting (turbulence dependent) force coefficient matrix
A_i^*	Quasi-static flutter derivatives for self-excited moment ($i = 1, 2 \ldots 6$)
$\boldsymbol{A}_\Delta$	Motion-dependent force coefficient matrix of structural displacements
$\boldsymbol{A}_{\dot{\Delta}}$	Motion-dependent force coefficient matrix of structural velocities
$\boldsymbol{A}_{i,axial}$	Separate axial force contribution to $\boldsymbol{A}_i$, for $\boldsymbol{i} = \Delta, \dot{\Delta}, b$
$\boldsymbol{A}_{Scanlan,\Delta}$	Alternative formulation of $\boldsymbol{A}_\Delta$, using Scanlan's flutter derivatives
$\boldsymbol{A}_{Scanlan,\dot{\Delta}}$	Alternative formulation of $\boldsymbol{A}_{\dot{\Delta}}$, using Scanlan's flutter derivatives
B	Cross-section width
$\boldsymbol{B}$	Diagonal matrix: $diag(B, B, B, B^2, B^2 B^2)$
$\boldsymbol{B}_{Lnw}$	Diagonal matrix: $diag(H, 0, B, 0, B^2, 0)$ (where the drag is normalized by H)
C, $\boldsymbol{C}$	Aerodynamic coefficient C. Vector of aerodynamic coefficients $\boldsymbol{C}$. C_i is in the i-axis (e.g. C_{X_u}). $\boldsymbol{C}_i$ is in the i-system (e.g. $\boldsymbol{C}_{Gw}$). $\tilde{C}$ and $\tilde{\boldsymbol{C}}$ depend on e.g. $(\tilde{\beta}, \tilde{\theta})$. $\tilde{\tilde{C}}$ and $\tilde{\tilde{\boldsymbol{C}}}$ depend on e.g. $(\tilde{\tilde{\beta}}, \tilde{\tilde{\theta}})$
C', $\boldsymbol{C}'$	Derivative of C or $\boldsymbol{C}$ with respect to θ_{yz}
C'^{β}, $\boldsymbol{C}'^{\beta}$	Partial derivative of C or $\boldsymbol{C}$ with respect to β
C'^{θ}, $\boldsymbol{C}'^{\theta}$	Partial derivative of C or $\boldsymbol{C}$ with respect to θ
$\hat{\boldsymbol{C}}$	Modal damping matrix
$\boldsymbol{C}^G$	Global damping matrix (for all nodes)
$\boldsymbol{C}_{AE}$	Aerodynamic damping matrix (for each element)
$\boldsymbol{C}_{AE}^G$	Global aerodynamic damping matrix (for all nodes)
$\boldsymbol{C}_S^G$	Global structural damping matrix (for all nodes)
$\tilde{\boldsymbol{f}}_{ad}$	Aerodynamic forces per unit length (due to $\boldsymbol{f}_{mean}$ and $\tilde{\boldsymbol{f}}_b$)
$\tilde{\tilde{\boldsymbol{f}}}_{ad}$	Aerodynamic forces per unit length (due to $\boldsymbol{f}_{mean}$ and $\tilde{\tilde{\boldsymbol{f}}}_b$)
$\tilde{\boldsymbol{f}}_b$	Buffeting forces per unit length (due to turbulence)
$\tilde{\tilde{\boldsymbol{f}}}_b$	Buffeting forces per unit length (due to turbulence and structural motions)
$\boldsymbol{f}_{i,axial}$	Separate axial force contribution to $\boldsymbol{f}_i$, for $\boldsymbol{i} = ad, b, mean$
$\boldsymbol{f}_{mean}$	Mean wind forces per unit length
$\tilde{\boldsymbol{F}}_{ad}$	Aerodynamic forces ($\tilde{\boldsymbol{F}}_{ad} = L\tilde{\boldsymbol{f}}_{ad}$)
$\boldsymbol{F}_b^G$	Global buffeting force vector (for all nodes)
H	Cross-section height
H_i^*	Quasi-static flutter derivatives for self-excited lift ($i = 1, 2 \ldots 6$)
$\hat{\boldsymbol{H}}$	Modal frequency response function matrix
k	Reduced frequency ($k = B\omega / U$)
$\boldsymbol{K}^G$	Global stiffness matrix (for all nodes)
$\hat{\boldsymbol{K}}$	Modal stiffness matrix
$\boldsymbol{K}_{AE}$	Aerodynamic stiffness matrix (for each element)
$\boldsymbol{K}_{AE}^G$	Global aerodynamic stiffness matrix (for all nodes)
$\boldsymbol{K}_S^G$	Global structural stiffness matrix (for all nodes)
L	Element length
$\boldsymbol{M}^G$	Global mass matrix (for all nodes)
$\hat{\boldsymbol{M}}$	Modal mass matrix
N_M	Number of modes
N_N	Number of nodes
$\boldsymbol{P}_b$	Coefficient matrix of buffeting forces (for each element)
$\boldsymbol{P}_b^G$	Global coefficient matrix of buffeting forces (for all nodes)
$\boldsymbol{P}_b^{G^*}$	Complex conjugate of $\boldsymbol{P}_b^G$
P_i^*	Quasi-static flutter derivatives for self-excited drag ($i = 1, 2 \ldots 6$)
$\boldsymbol{R}_i(\gamma)$	Rotation matrix around a generic i-axis, by a generic angle γ
S, $\tilde{S}$, $\tilde{\tilde{S}}$	Sign functions: $sgn(\cos\beta)$, $sgn(\cos\tilde{\beta})$, $sgn(\cos\tilde{\tilde{\beta}})$
$\boldsymbol{S}_\Delta$	Auto spectral density matrix of the nodal displacement response
$\boldsymbol{S}_{\Delta\Delta}$	Cross spectral density matrix of the nodal displacement response
$\boldsymbol{S}_{\hat{\eta}\hat{\eta}}$	Cross spectral density matrix of the modal displacement response
$\boldsymbol{S}_{aa}$	Cross spectral density matrix of the fluctuating wind components
$\boldsymbol{S}_{\hat{F}\hat{F}}$	Cross spectral density matrix of the modal buffeting loads
t	Time (position in time)
$\boldsymbol{T}_{ji}$	Transformation matrix from the coordinate system i to the coordinate system j
u	Turbulence component along the mean wind
$\tilde{\tilde{u}}$	Relative velocity between u and the moving bridge
U, U_i, $\boldsymbol{U}_i$	Mean wind speed U; mean wind projection in the i-axis or i-plane U_i; mean wind vector in the i-system $\boldsymbol{U}_i$
$\tilde{U}$, $\tilde{U}_i$, $\tilde{\boldsymbol{U}}_i$	Local instantaneous wind speed $\tilde{U}$ (turbulence dependent); local instantaneous wind projection in the i-axis or i-plane $\tilde{U}_i$, or vector in the i-system $\tilde{\boldsymbol{U}}_i$
$\tilde{\tilde{U}}$, $\tilde{\tilde{U}}_i$, $\tilde{\tilde{\boldsymbol{U}}}_i$	Local instantaneous relative wind speed $\tilde{\tilde{U}}$ (turbulence and

motion dependent); local instantaneous relative wind projection in the i-axis or i-plane $\tilde{\tilde{U}}_i$, or vector in the i-system $\tilde{\tilde{\boldsymbol{U}}}_i$
v Horizontal turbulence component across the mean wind
$\tilde{\tilde{v}}$ Relative velocity between v and the moving bridge
v_i A generic vector in the coordinate system i
w Upward turbulence component, perpendicular to u and v
$\tilde{\tilde{w}}$ Relative velocity between w and the moving bridge

Accents/superscripts/styles
$\tilde{\ }$ Time-varying quantity due to turbulence
$\tilde{\tilde{\ }}$ Time-varying quantity due to turbulence (if applicable) and structural motions
$\dot{\ }$ First time derivative
$\ddot{\ }$ Second time derivative
$\hat{\ }$ Modal quantity
^{G} Global quantity, relative to all nodes/elements and DOF (omitted when there is no ambiguity between nodal/elemental and global quantities (e.g. $\boldsymbol{S}_{\Delta\Delta}$))
boldface Variables in **bold** represent vectors and matrices

Acronyms
1D, 2D or 3D 1-, 2-, or 3-dimensional (in space)
CFD Computational fluid dynamics
DOF Degrees-of-freedom
FEM Finite element method

Coordinate systems and respective axes
$Gs\ (\boldsymbol{X},\boldsymbol{Y},\boldsymbol{Z})$ Global structural $(\boldsymbol{X},\boldsymbol{Y},\boldsymbol{Z},\boldsymbol{rX},\boldsymbol{rY},\boldsymbol{rZ})$
$Ls\ (\boldsymbol{x},\boldsymbol{y},\boldsymbol{z})$ Local (static) structural $(\boldsymbol{x},\boldsymbol{y},\boldsymbol{z},\boldsymbol{rx},\boldsymbol{ry},\boldsymbol{rz})$
$\tilde{\tilde{Ls}}\ (\tilde{\tilde{\boldsymbol{x}}},\tilde{\tilde{\boldsymbol{y}}},\tilde{\tilde{\boldsymbol{z}}})$ Local dynamic structural $(\tilde{\tilde{\boldsymbol{x}}},\tilde{\tilde{\boldsymbol{y}}},\tilde{\tilde{\boldsymbol{z}}},\tilde{\tilde{\boldsymbol{rx}}},\tilde{\tilde{\boldsymbol{ry}}},\tilde{\tilde{\boldsymbol{rz}}})$
$Gw\ (\boldsymbol{X_u},\boldsymbol{Y_v},\boldsymbol{Z_w})$ Global mean wind $(\boldsymbol{X_u},\boldsymbol{Y_v},\boldsymbol{Z_w},\boldsymbol{rX_u},\boldsymbol{rY_v},\boldsymbol{rZ_w})$
$\widetilde{Lw}(\boldsymbol{X}_{\tilde{U}},\boldsymbol{Y}_{\tilde{U}},\boldsymbol{Z}_{\tilde{U}})$ Local instantaneous wind $(\boldsymbol{X}_{\tilde{U}},\boldsymbol{Y}_{\tilde{U}},\boldsymbol{Z}_{\tilde{U}},\boldsymbol{rX}_{\tilde{U}},\boldsymbol{rY}_{\tilde{U}},\boldsymbol{rZ}_{\tilde{U}})$
$\widetilde{\widetilde{Lw}}\ (\boldsymbol{X}_{\tilde{\tilde{U}}},\boldsymbol{Y}_{\tilde{\tilde{U}}},\boldsymbol{Z}_{\tilde{\tilde{U}}})$ Local instantaneous relative wind$(\boldsymbol{X}_{\tilde{\tilde{U}}},\boldsymbol{Y}_{\tilde{\tilde{U}}},\boldsymbol{Z}_{\tilde{\tilde{U}}},\boldsymbol{rX}_{\tilde{\tilde{U}}},\boldsymbol{rY}_{\tilde{\tilde{U}}},\boldsymbol{rZ}_{\tilde{\tilde{U}}})$
$Lnw\ (\boldsymbol{D},\boldsymbol{A},\boldsymbol{L})$ Local mean normal wind $(\boldsymbol{D},\boldsymbol{A},\boldsymbol{L},\boldsymbol{rD},\boldsymbol{M},\boldsymbol{rL})$
$\widetilde{Lnw}\ (\tilde{\boldsymbol{D}},\tilde{\boldsymbol{A}},\tilde{\boldsymbol{L}})$ Local instantaneous normal wind $(\tilde{\boldsymbol{D}},\tilde{\boldsymbol{A}},\tilde{\boldsymbol{L}},\widetilde{\boldsymbol{rD}},\tilde{\boldsymbol{M}},\widetilde{\boldsymbol{rL}})$
$\widetilde{\widetilde{Lnw}}\ (\tilde{\tilde{\boldsymbol{D}}},\tilde{\tilde{\boldsymbol{A}}},\tilde{\tilde{\boldsymbol{L}}})$ Local instantaneous relative normal wind $(\tilde{\tilde{\boldsymbol{D}}},\tilde{\tilde{\boldsymbol{A}}},\tilde{\tilde{\boldsymbol{L}}},\widetilde{\widetilde{\boldsymbol{rD}}},\tilde{\tilde{\boldsymbol{M}}},\widetilde{\widetilde{\boldsymbol{rL}}})$

Fig. 1a. A planned floating bridge solution for Bjørnafjorden, Norway.

tent outcomes. A simplified buffeting theory for turbulence using the *cosine rule* is proposed in (Xie et al., 1991) with reasonable agreement with experimental results. In (Tanaka and Davenport, 1982), the *cosine rule* underestimated the response of taut strip models in boundary layer turbulence, under highly turbulent wind. In (Zhu, 2002), Tsing Ma suspension bridge experiences its maximum lateral buffeting response when the mean wind has a yaw angle β of $+5^\circ$ and an inclination angle $\theta = -2.5^\circ$. This response is practically constant within a β range of $\pm 15^\circ$, which diverges from the *cosine rule* estimation. The maximum vertical response was observed at $\beta = \pm 12^\circ$ and $\theta = 4^\circ$. In (Wang et al., 2011), a numerical *cosine rule* analysis, when compared with the measured response of the Runyang suspension bridge, showed somewhat underestimated torsional and vertical responses, but several other uncertainty sources were also present. In (Huang et al., 2012), sectional model tests were compared with numerical analyses of two girders with rectangular cross-sections with B/H (width to height) ratios of 5 and 10. Significant underestimations of the response when using the *cosine rule* were observed, especially for the $B/H = 10$ case, where, also, the minimum flutter speed was observed for $\beta = 20^\circ$. For bridges under construction, where the girder has one or both ends free and exposed to the wind, additional flow asymmetries are to be expected. For such cases, significant differences were observed by (Kimura and Tanaka, 1992), even when complementing the *cosine rule* with a *sine rule*, (Li et al., 2016) saw larger wind loads for β between 10° and 30°, (Jian et al., 2020) for β between 0° and 30°, whereas (Scanlan, 1993) reported a reasonable match between calculated and measured responses when carefully assessing several aerodynamic and structural parameters.

It can be concluded that previous literature, despite some inconsistencies, has shown that the maximum wind response can occur under skew winds and that a simplified *cosine rule* analysis can underestimate the response. These findings, which only concern straight bridges, raise further questions for a curved line-like structure such as the planned bridge for Bjørnafjorden in Fig. 1a, where its curved design creates a natural variation of the mean yaw angle β along the bridge, as exemplified in Fig. 1b. Additionally, its grade (slope) adds a variation of the mean inclination angle θ, for any given global mean wind direction.

Complex bridge geometries, such as the one illustrated, also draw the need to reformulate previous buffeting theories, which have been mainly developed for straight bridges. A careful and comprehensive use of coordinate systems, consistent for all mean wind directions when possible, can lead to simpler and clearer expressions. An intuitive and systematic use of transformation matrices ensures that all DOF (degrees-of-freedom) and motion-dependencies are handled correctly.

The present skew wind buffeting theory consists of a partial revision and a complement to the pioneering doctoral thesis by Prof. Le-Dong Zhu (2002) where the present work was based. The theory by Zhu is also summarized in (Xu and Zhu, 2005; Zhu and Xu, 2005) and in (Xu, 2013). The main changes introduced in this revised version are

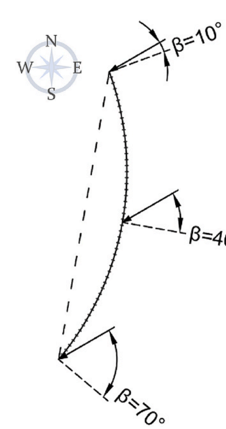

Fig. 1b. Plan view sketch. Example of β variation for one mean wind direction.

summarized in the Appendix.

The present theory addresses the 3D load effects of the wind turbulence as well as the motion-dependent forces that arise from the interaction between the turbulent wind and the moving structure, for an arbitrary mean wind direction. A quasi-steady (frequency independent) motion-dependent force formulation, considering all six DOF, is presented first. This formulation should only be used whenever the preferred unsteady (frequency dependent) estimates are not available for the different skew angles. An alternative quasi-steady formulation using only the three typical DOF in Scanlan's flutter derivatives (Scanlan and Tomo, 1971) is also provided, which can then be readily adapted to an unsteady format.

Despite the criticism, there are no general and well-established alternatives to the *cosine rule* whenever the yaw-dependency of the aerodynamic coefficients is unknown. To facilitate simplified preliminary studies, as well as for comparison purposes, the present theory also includes a 2D approach as a more rigorous generalization of the *cosine rule*. Whereas the *cosine rule* assumes the bridge and the wind to be both horizontal and ignores motions outside the normal plane, the 2D approach presented allows for any mean yaw angle and mean inclination angle, for both buffeting and motion-dependent forces, including motions in all degrees-of-freedom.

Linearized forms of the relevant forces and variables for both 3D and 2D approaches are achieved through numerous multivariate Taylor series approximations and extensive mathematical simplifications. The non-linear and linearized forms are presented separately to facilitate typical time-domain and frequency-domain analyses of the bridge buffeting response. Wind loads are presented as functions of the turbulence in global wind coordinates (i.e. as a function of u, v and w) to also facilitate wind field simulations in the time-domain and allow the use of available spectral and three-dimensional coherence models of the wind turbulence.

The computer algebra systems *SymPy (v1.6.2)* (a *Python* library for symbolic mathematics) and *Wolfram Mathematica (v12.1)* were both used to help deduce, linearize, simplify and verify the present theory.

2. Background concepts, conventions and terms

To represent a general case of arbitrary wind and bridge orientations it is convenient to establish a set of right-handed Cartesian coordinate systems which can be chosen freely by the user, as well as the associated transformation matrices.

First, a global wind $(\boldsymbol{X_u}, \boldsymbol{Y_v}, \boldsymbol{Z_w})$ coordinate system is introduced in Fig. 2a and Fig. 2b, hereby denoted *Gw*. The axis $\boldsymbol{X_u}$ describes the direction of the mean wind, with a mean velocity U, and the along-wind turbulence, with velocity u. $\boldsymbol{Y_v}$ describes the direction of the across-wind horizontal turbulence v and $\boldsymbol{Z_w}$ describes the direction of the turbulence component w, such that $\boldsymbol{Z_w} = \boldsymbol{X_u} \times \boldsymbol{Y_v}$ (cross-product). The global structural *Gs* $(\boldsymbol{X}, \boldsymbol{Y}, \boldsymbol{Z})$ coordinate system adopted is also illustrated in Fig. 2a.

The local structural *Ls* $(\boldsymbol{x}, \boldsymbol{y}, \boldsymbol{z})$ coordinate system adopted (for each element) is illustrated in Fig. 2b, along with the main angles in the context of skew winds, β and θ, hereby defined as follows:

- β – the yaw angle, is defined as the angle between the local $\boldsymbol{y}$-axis and the mean wind vector $\boldsymbol{X_u}$ projection onto the $\boldsymbol{xy}$-plane, in the half-open interval $]-180^\circ, 180^\circ]$, with a positive sign if the projection of $\boldsymbol{X_u}$ on the $\boldsymbol{x}$-axis has opposite direction to $\boldsymbol{x}$.
- θ – the inclination angle, is defined as the angle between the bridge local $\boldsymbol{xy}$-plane and the $\boldsymbol{X_u}$, in the open interval $]-90^\circ, 90^\circ[$, with a positive sign if the projection of $\boldsymbol{X_u}$ on the z-axis has the same direction as z.

The same angles, when measured with respect to the global *Gs* coordinate system, are called β_G and θ_G, and can be directly related to the wind cardinal directions.

Analogous to Earth's longitude and latitude, respectively, β and θ describe all possible wind directions, provided that the two singularities at $\theta = \pm 90^\circ$ can be ignored. The aerodynamic coefficients, $\boldsymbol{C}(\beta, \theta)$, necessary to estimate the wind loads, can then be described at each bridge element as functions of both these angles. In the *Gw* system for instance, when all 6 DOF are considered, $\boldsymbol{C}_{Gw}(\beta, \theta) = [C_{X_u}, C_{Y_v}, C_{Z_w}, C_{rX_u}, C_{rY_v}, C_{rZ_w}]^T$.

Any coordinate system can now be conveniently expressed through transformations or rotations of the previously defined systems. A transformation matrix is the transpose, and also the inverse, of a rotation matrix, as both are orthogonal.

To transform any column vector $\boldsymbol{v}_{XYZ}$, represented in a coordinate system $(\boldsymbol{X}, \boldsymbol{Y}, \boldsymbol{Z})$, into the same vector $\boldsymbol{v}_{xyz}$, represented in another coordinate system $(\boldsymbol{x}, \boldsymbol{y}, z)$ with the same origin, eqs. (1)–(3) can be used. $\boldsymbol{T}_{xyzXYZ}$ is a generic transformation matrix. γ_{ij} is the angle between two vectors $\boldsymbol{i}$ and $\boldsymbol{j}$.

$$\boldsymbol{v}_{xyz} = \boldsymbol{T}_{xyzXYZ}\, \boldsymbol{v}_{XYZ} \tag{1}$$

$$\boldsymbol{T}_{xyzXYZ} = \begin{bmatrix} \cos(\gamma_{xX}) & \cos(\gamma_{xY}) & \cos(\gamma_{xZ}) \\ \cos(\gamma_{yX}) & \cos(\gamma_{yY}) & \cos(\gamma_{yZ}) \\ \cos(\gamma_{zX}) & \cos(\gamma_{zY}) & \cos(\gamma_{zZ}) \end{bmatrix} = \boldsymbol{T}_{XYZxyz}^T \tag{2}$$

$$\cos(\gamma_{ij}) = \frac{\boldsymbol{i} \cdot \boldsymbol{j}}{\|\boldsymbol{i}\| \cdot \|\boldsymbol{j}\|} \tag{3}$$

In the 6 DOF format mentioned henceforth, e.g. $(\boldsymbol{x}, \boldsymbol{y}, z, \boldsymbol{rx}, \boldsymbol{ry}, \boldsymbol{rz})$, each of the three additional r-axes represents a rotation around the axis that its second letter refers to. To expand to this format, the vectors in eq. (1) can be replaced by their 6 DOF counterparts, such that the 6×6 transformation matrix follows eq. (4). All 6 DOF can then be included, even though only the first 3 are usually mentioned, for the sake of simplicity.

$$\boldsymbol{T}_{xyzXYZ}^{(6\times6)} = \begin{bmatrix} \boldsymbol{T}_{xyzXYZ}^{(3\times3)} & \boldsymbol{0} \\ \boldsymbol{0} & \boldsymbol{T}_{xyzXYZ}^{(3\times3)} \end{bmatrix}, \textit{with } \boldsymbol{0} = \begin{bmatrix} 0 & 0 & 0 \\ 0 & 0 & 0 \\ 0 & 0 & 0 \end{bmatrix} \tag{4}$$

Transformation matrices also have the properties presented in eqs. (5) and (6), where the subscripts $_{S1}$, $_{S2}$ and $_{S3}$ are used to denote three different coordinate systems and where for instance $\boldsymbol{T}_{S3S1}$ denotes a transformation from $_{S1}$ to $_{S3}$.

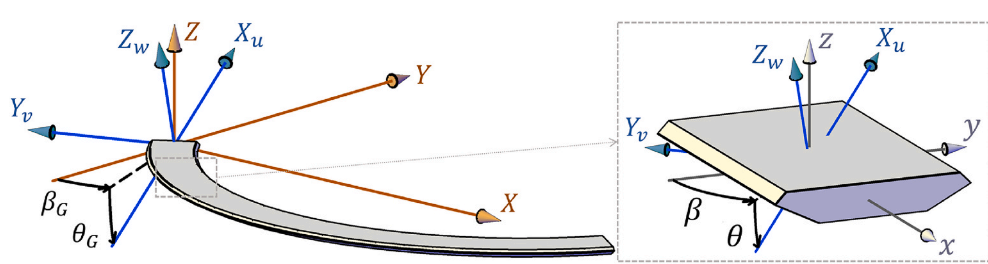

Fig. 2. a) Global wind – *Gw* – $(\boldsymbol{X_u}, \boldsymbol{Y_v}, \boldsymbol{Z_w})$ and global structural – *Gs* – $(\boldsymbol{X}, \boldsymbol{Y}, \boldsymbol{Z})$ coordinate systems; global mean yaw angle β_G and global mean inclination angle θ_G. **b)** Global wind – *Gw* – $(\boldsymbol{X_u}, \boldsymbol{Y_v}, \boldsymbol{Z_w})$ and local structural – *Ls* – $(\boldsymbol{x}, \boldsymbol{y}, z)$ coordinate systems; local mean yaw angle β and local mean inclination angle θ.

$$\boldsymbol{T}_{S2S1} = \boldsymbol{T}_{S1S2}^{-1} = \boldsymbol{T}_{S1S2}^{T} \tag{5}$$

$$\boldsymbol{T}_{S3S1} = \boldsymbol{T}_{S3S2}\,\boldsymbol{T}_{S2S1} \tag{6}$$

A transformation matrix can be also obtained through meaningful rotations from a known system to another. Three elemental rotation matrices are presented in eqs. (7)–(9). Each one represents a rotation around an axis, by a generic angle γ, following the right-hand rule.

$$\boldsymbol{R}_X(\gamma) = \begin{bmatrix} 1 & 0 & 0 \\ 0 & \cos(\gamma) & -\sin(\gamma) \\ 0 & \sin(\gamma) & \cos(\gamma) \end{bmatrix} = \boldsymbol{T}_X(\gamma)^T \tag{7}$$

$$\boldsymbol{R}_Y(\gamma) = \begin{bmatrix} \cos(\gamma) & 0 & \sin(\gamma) \\ 0 & 1 & 0 \\ -\sin(\gamma) & 0 & \cos(\gamma) \end{bmatrix} = \boldsymbol{T}_Y(\gamma)^T \tag{8}$$

$$\boldsymbol{R}_Z(\gamma) = \begin{bmatrix} \cos(\gamma) & -\sin(\gamma) & 0 \\ \sin(\gamma) & \cos(\gamma) & 0 \\ 0 & 0 & 1 \end{bmatrix} = \boldsymbol{T}_Z(\gamma)^T \tag{9}$$

Chained rotations are then composed of two or more of these elemental rotations. They can be extrinsic (rotations around the original coordinate system axes, which remain fixed during all rotations, when each rotation matrix is pre-multiplied by the next rotation matrix), or intrinsic (rotations around the axes that are solidary to the rotating object, which change for each rotation, when each rotation matrix is post-multiplied by the next rotation matrix). To conveniently obtain the necessary transformation matrices, intrinsic chained rotations are adopted.

Based on Fig. 2a, the fixed *Gw* system can be obtained from given values of β_G and θ_G, by first rotating the *Gs* system around the $\boldsymbol{Z}$-axis by the angle $\pi/2 + \beta_G$, and then around the newly obtained axis $\boldsymbol{Y}_v$ by the negative angle θ_G, as shown in eq. (10).

$$\boldsymbol{T}_{GwGs} = \left(\boldsymbol{R}_Z(\pi/2 + \beta_G)\boldsymbol{R}_Y(-\theta_G)\right)^T = \begin{bmatrix} -\cos(\theta_G)\sin(\beta_G) & \cos(\theta_G)\cos(\beta_G) & \sin(\theta_G) \\ -\cos(\beta_G) & -\sin(\beta_G) & 0 \\ \sin(\theta_G)\sin(\beta_G) & -\sin(\theta_G)\cos(\beta_G) & \cos(\theta_G) \end{bmatrix} \tag{10}$$

To obtain the transformation matrices $\boldsymbol{T}_{LsGs}$, between the global structural and the local structural coordinate systems (one $\boldsymbol{T}_{LsGs}$ for each finite element), the generic eqs. (2) and (3) can be used, after defining all local $\boldsymbol{x}$, $\boldsymbol{y}$ and $\boldsymbol{z}$ axes. When a static analysis precedes the buffeting analysis, the axes of the *Ls* systems and relevant transformation matrices should be updated accordingly. It should be noted that the deck rotation due to the static wind may play an important role.

The "for each element" and "for each node" representations used throughout the text are not strict. They are often interchangeable, provided that the principles of finite element modelling are followed (see e.g. (Bathe, 2006; Hutton, 2004)).

The mean wind speed U, mean yaw angle β and mean inclination angle θ have their time-varying counterparts $\tilde{U}$, $\tilde{\beta}$ and $\tilde{\theta}$ which consider the instantaneous wind turbulence components u, v and w at each time instant. The turbulence-dependent quantities are denoted "instantaneous" and represented by one tilde accent. Subscripts are used to indicate the coordinate systems (e.g. *Ls*, *Gw*) in which these quantities are represented as vectors, or the axes (e.g. $\boldsymbol{x}$, $\boldsymbol{y}$, $\boldsymbol{z}$) or plane (e.g. $\boldsymbol{xy}$) they are projected onto. These quantities can be obtained through eqs. (11)–(20), for each element.

Mean quantities:		Instantaneous quantities:	
$\boldsymbol{U}_{Gw} = [U,\ 0,\ 0]^T$	(11)	$\tilde{\boldsymbol{U}}_{Gw} = [U+u,\ v,\ w]^T$	(12)
$\boldsymbol{U}_{Ls} = [U_x,\ U_y,\ U_z]^T = \boldsymbol{T}_{LsGw}\,\boldsymbol{U}_{Gw}$	(13)	$\tilde{\boldsymbol{U}}_{Ls} = [\tilde{U}_x,\ \tilde{U}_y,\ \tilde{U}_z]^T = \boldsymbol{T}_{LsGw}\,\tilde{\boldsymbol{U}}_{Gw}$	(14)
$U_{xy} = \sqrt{{U_x}^2 + {U_y}^2}$	(15)	$\tilde{U}_{xy} = \sqrt{\tilde{U}_x^2 + \tilde{U}_y^2}$	(16)
$\beta = -\arccos(U_y/U_{xy})\,sgn(U_x)$	(17)	$\tilde{\beta} = -\arccos(\tilde{U}_y/\tilde{U}_{xy})sgn(\tilde{U}_x)$	(18)
$\theta = \arcsin(U_z/U)$	(19)	$\tilde{\theta} = \arcsin(\tilde{U}_z/\tilde{U})$	(20)

Where $\boldsymbol{T}_{LsGw} = \boldsymbol{T}_{LsGs}\boldsymbol{T}_{GsGw} = \boldsymbol{T}_{LsGs}\boldsymbol{T}_{GwGs}^T$ and *sgn* is the sign function. Alternatively, $\beta = atan2(-U_x, U_y)$ and $\tilde{\beta} = atan2(-\tilde{U}_x, \tilde{U}_y)$ can be used, where *atan2* is the "2-argument arctangent" function. The instantaneous wind speed $\tilde{U}$ is obtained by eq. (21).

$$\tilde{U} = \left\|\tilde{\boldsymbol{U}}_{Ls}\right\| = \left\|\tilde{\boldsymbol{U}}_{Gw}\right\| = \sqrt{(U+u)^2 + v^2 + w^2} \tag{21}$$

Next, motion-dependent (or simply "relative") variables are introduced which, in addition to the effects of turbulence (when applicable), also consider the effects of the structure in motion and are represented by a double tilde accent. The turbulence components u, v and w, when accounting for the relative velocity between the wind and the moving structure are denoted $\tilde{\tilde{u}}$, $\tilde{\tilde{v}}$ and $\tilde{\tilde{w}}$ and are defined in eqs. (22)–(24). Δ is the structural displacement vector (e.g. at the centre of a given element) and its time-derivative $\dot{\Delta}$ is the vector of structural velocities. They can be conveniently represented at the axes $\boldsymbol{X}_u$, $\boldsymbol{Y}_v$ and $\boldsymbol{Z}_w$ of the *Gw* system and simply obtained by $\dot{\Delta}_{Gw} = \boldsymbol{T}_{GwLs}\dot{\Delta}_{Ls}$, i.e., in a 3 DOF format, $[\dot{\Delta}_{X_u}, \dot{\Delta}_{Y_v}, \dot{\Delta}_{Z_w}]^T = \boldsymbol{T}_{GwLs}[\dot{\Delta}_x, \dot{\Delta}_y, \dot{\Delta}_z]^T$. The instantaneous relative wind speed is given by eq. (25), whereas its vector representations in the *Gw* system and in the local dynamic structural $\underset{\approx}{Ls}$ system (solidary with the rotating body) are given in eqs. (26) and (27).

Motion-dependent quantities:	
$\tilde{\tilde{u}} = u - \dot{\Delta}_{X_u}$	(22)
$\tilde{\tilde{v}} = v - \dot{\Delta}_{Y_v}$	(23)
$\tilde{\tilde{w}} = w - \dot{\Delta}_{Z_w}$	(24)
$\tilde{\tilde{U}} = \sqrt{(U+\tilde{\tilde{u}})^2 + \tilde{\tilde{v}}^2 + \tilde{\tilde{w}}^2}$	(25)
$\tilde{\tilde{\boldsymbol{U}}}_{Gw} = [U+\tilde{\tilde{u}},\ \tilde{\tilde{v}},\ \tilde{\tilde{w}}]^T$	(26)
$\tilde{\tilde{\boldsymbol{U}}}_{\underset{\approx}{Ls}} = [\tilde{\tilde{U}}_{\underset{\approx}{x}},\ \tilde{\tilde{U}}_{\underset{\approx}{y}},\ \tilde{\tilde{U}}_{\underset{\approx}{z}}]^T = \boldsymbol{T}_{\underset{\approx}{Ls}Ls}\,\boldsymbol{T}_{LsGw}\tilde{\tilde{\boldsymbol{U}}}_{Gw}$	(27)

To obtain the transformation from the static structure to the dynamic (rotating) structure $\boldsymbol{T}_{\underset{\approx}{Ls}Ls}$ at each time step, three chained rotations can be performed if the rotations are assumed small, as in eq. (28). Moreover, when $\boldsymbol{T}_{\underset{\approx}{Ls}Ls}$ is linearized with respect to Δ_{rx}, Δ_{ry} and Δ_{rz}, these three elemental rotations become commutative and $\boldsymbol{T}_{\underset{\approx}{Ls}Ls}$ gets further simplified into eq. (29).

$$\boldsymbol{T}_{\underset{\approx}{Ls}Ls} \approx \left(\boldsymbol{R}_X(\Delta_{rx})\boldsymbol{R}_Y(\Delta_{ry})\boldsymbol{R}_Z(\Delta_{rz})\right)^T \tag{28}$$

$$\left(\boldsymbol{R}_X(\Delta_{rx})\boldsymbol{R}_Y(\Delta_{ry})\boldsymbol{R}_Z(\Delta_{rz})\right)^T \approx \begin{bmatrix}1 & \Delta_{rz} & -\Delta_{ry}\\ -\Delta_{rz} & 1 & \Delta_{rx}\\ \Delta_{ry} & -\Delta_{rx} & 1\end{bmatrix} \quad (29)$$

Given that $\tilde{\tilde{U}}_{\tilde{\tilde{xy}}} = \sqrt{\tilde{\tilde{U}}^2_{\tilde{\tilde{x}}} + \tilde{\tilde{U}}^2_{\tilde{\tilde{y}}}}$, the instantaneous motion-dependent counterparts of β and θ can be obtained from eqs. (30) and (31).

$$\tilde{\tilde{\beta}} = -\arccos(\tilde{\tilde{U}}_{\tilde{\tilde{y}}}/\tilde{\tilde{U}}_{\tilde{\tilde{xy}}})\,sgn(\tilde{\tilde{U}}_{\tilde{\tilde{x}}}) \quad (30)$$

$$\tilde{\tilde{\theta}} = \arcsin(\tilde{\tilde{U}}_{\tilde{\tilde{z}}}/\tilde{\tilde{U}}) \quad (31)$$

Two additional right-handed orthogonal coordinate systems are adopted, namely the local instantaneous wind $\widetilde{Lw}(X_{\tilde{U}}, Y_{\tilde{U}}, Z_{\tilde{U}})$ and the local relative instantaneous wind $\tilde{\tilde{Lw}}(X_{\tilde{\tilde{U}}}, Y_{\tilde{\tilde{U}}}, Z_{\tilde{\tilde{U}}})$, described by the conditions in eqs. (32) and (33). $\tilde{U}$ and $\tilde{\tilde{U}}$ are represented in $X_{\tilde{U}}$ and $X_{\tilde{\tilde{U}}}$ respectively.

$$X_{\tilde{U}} = \tilde{\boldsymbol{U}}_{Gw}/\|\tilde{\boldsymbol{U}}_{Gw}\|;\quad Y_{\tilde{U}} \parallel \boldsymbol{xy}\text{-plane} \wedge sgn(Z_{\tilde{U}}\cdot z) > 0;\quad Z_{\tilde{U}} = X_{\tilde{U}} \times Y_{\tilde{U}} \quad (32)$$

$$X_{\tilde{\tilde{U}}} = \tilde{\tilde{\boldsymbol{U}}}_{Gw}/\|\tilde{\tilde{\boldsymbol{U}}}_{Gw}\|;\quad Y_{\tilde{\tilde{U}}} \parallel \tilde{\tilde{\boldsymbol{xy}}}\text{-plane} \wedge sgn(Z_{\tilde{\tilde{U}}}\cdot \tilde{\tilde{z}}) > 0;\quad Z_{\tilde{\tilde{U}}} = X_{\tilde{\tilde{U}}} \times Y_{\tilde{\tilde{U}}} \quad (33)$$

These two systems help represent the aerodynamic forces $\tilde{\boldsymbol{f}}_{ad,\widetilde{Lw}}$ and $\tilde{\tilde{\boldsymbol{f}}}_{ad,\tilde{\tilde{Lw}}}$ and the respective coefficients $\tilde{\boldsymbol{C}}_{\widetilde{Lw}}(\tilde{\beta},\tilde{\theta})$ and $\tilde{\tilde{\boldsymbol{C}}}_{\tilde{\tilde{Lw}}}(\tilde{\tilde{\beta}},\tilde{\tilde{\theta}})$ at each time instant, as shown in section 3.

A schematic comparison between the key mean, instantaneous and motion-dependent variables is illustrated in Fig. 3.

3. A 3D buffeting approach for skew winds

A 3D skew wind buffeting analysis requires information on aerodynamic coefficients $\boldsymbol{C}(\beta,\theta)$ that depend on both β and θ. These can be obtained through wind tunnel tests at different yaw angles or through three-dimensional CFD analyses.

3.1. Fluctuating wind forces due to turbulence

3.1.1. Non-linear forces

The vector of the six aerodynamic forces in the *Gs* system, for each element and at each time instant, can be simply expressed through eq. (34), using consistent (i.e. represented in a time-invariant system) aerodynamic coefficients $\tilde{\boldsymbol{C}}_{Ls}(\tilde{\beta},\tilde{\theta}) = [\tilde{C}_x, \tilde{C}_y, \tilde{C}_z, \tilde{C}_{rx}, \tilde{C}_{ry}, \tilde{C}_{rz}]^T$, which depend on the instantaneous $\tilde{\beta}$ and $\tilde{\theta}$.

$$\tilde{\boldsymbol{F}}_{ad,Gs} = L\tilde{\boldsymbol{f}}_{ad,Gs} = L\,\boldsymbol{T}_{GsLs}\tilde{\boldsymbol{f}}_{ad,Ls} = L\,\boldsymbol{T}_{GsLs}1/2\,\rho\tilde{U}^2\boldsymbol{B}\tilde{\boldsymbol{C}}_{Ls} \quad (34)$$

L is the element length. Uppercase $\boldsymbol{F}$ denotes forces and lowercase $\boldsymbol{f}$ denotes forces per unit length. ρ is the air density. $\boldsymbol{B} = diag(B,B,B,B^2,B^2,B^2)$ is a diagonal matrix where B is the real cross-section width.

It is however more common to express $\tilde{\boldsymbol{f}}_{ad}$ as a function of aerodynamic coefficients $\tilde{\boldsymbol{C}}_{\widetilde{Lw}}(\tilde{\beta},\tilde{\theta}) = [\tilde{C}_{X_{\tilde{U}}}, \tilde{C}_{Y_{\tilde{U}}}, \tilde{C}_{Z_{\tilde{U}}}, \tilde{C}_{rX_{\tilde{U}}}, \tilde{C}_{rY_{\tilde{U}}}, \tilde{C}_{rZ_{\tilde{U}}}]^T$ that are solidary with the instantaneous wind direction $\tilde{U}$. These forces must therefore be transformed, at each time step, from $\widetilde{Lw}$ to a consistent coordinate system, such as *Gw* (solidary with *U*), through $\boldsymbol{T}_{Gw\widetilde{Lw}}$, as expressed in eqs. (35)–(37).

$$\tilde{\boldsymbol{F}}_{ad,Gs} = L\,\boldsymbol{T}_{GsGw}\tilde{\boldsymbol{f}}_{ad,Gw} = L\,\boldsymbol{T}_{GsGw}\boldsymbol{T}_{Gw\widetilde{Lw}}1/2\,\rho\tilde{U}^2\boldsymbol{B}\tilde{\boldsymbol{C}}_{\widetilde{Lw}} \quad (35)$$

$$\boldsymbol{T}_{Gw\widetilde{Lw}} = \boldsymbol{T}_{GwLs}\,\boldsymbol{T}_{Ls\widetilde{Lw}} \quad (36)$$

$$\boldsymbol{T}_{Ls\widetilde{Lw}} = (\boldsymbol{R}_Y(\tilde{\theta})\,\boldsymbol{R}_Z(-\tilde{\beta}-\pi/2))^T \quad (37)$$

Note that all coefficients are normalized by B or B^2, for simplicity. The relation between both aerodynamic coefficient representations is expressed in eq. (38), and either or both can be used, as preferred.

$$\tilde{\boldsymbol{C}}_{Ls} = \boldsymbol{T}_{Ls\widetilde{Lw}}\tilde{\boldsymbol{C}}_{\widetilde{Lw}} \quad (38)$$

The aerodynamic forces, first obtained for each finite beam element, can be converted into forces at both local nodes of each element and then converted into global nodal forces, following standard FEM transformation techniques.

Aerodynamic forces $\tilde{\boldsymbol{f}}_{ad}$ are here defined as the sum of the mean wind forces $\boldsymbol{f}_{mean}$ and the time-varying buffeting forces $\tilde{\boldsymbol{f}}_b$, so the buffeting part can be retrieved from eq. (39) and linearized when convenient.

$$\tilde{\boldsymbol{f}}_{b,Gw} = \tilde{\boldsymbol{f}}_{ad,Gw} - \boldsymbol{f}_{mean,Gw} = \tilde{\boldsymbol{f}}_{ad,Gw} - 1/2\,\rho U^2\boldsymbol{BC}_{Gw} \quad (39)$$

Where $\boldsymbol{C}_{Gw}(\beta,\theta)$ depends on the mean β and θ.

3.1.2. Linearizations

Presuming that the time-varying velocities u, v and w are small compared to U, then the local instantaneous yaw angle $\tilde{\beta}$, defined in eq. (18), can be represented as a function of U, u, v, w, β and θ. By performing a first order Taylor expansion with respect to u, v and w, as in eq. (40), by conveniently separating the two cases of $\beta \in]-180^\circ, 0^\circ]$ and $\beta \in [0^\circ, 180^\circ]$, and by considering that $\theta \in]-90^\circ, 90^\circ[$, numerous simplifications can be made.

$$\tilde{\beta}(U,u,v,w,\beta,\theta) \approx \tilde{\beta}_{u,v,w=0} + \tilde{\beta}'^{u}_{u,v,w=0}u + \tilde{\beta}'^{v}_{u,v,w=0}v + \tilde{\beta}'^{w}_{u,v,w=0}w \quad (40)$$

Then, equally for both cases of the β-interval, the linear approximation in eq. (41) is obtained. A similar process can be done for $\tilde{\theta}$, $\boldsymbol{T}_{Gw\widetilde{Lw}}$ and $\tilde{U}^2$, leading to eqs. (42)–(44).

$$\tilde{\beta} = \beta + \widetilde{\Delta\beta} \approx \beta + \frac{v}{U\cos\theta} \quad (41)$$

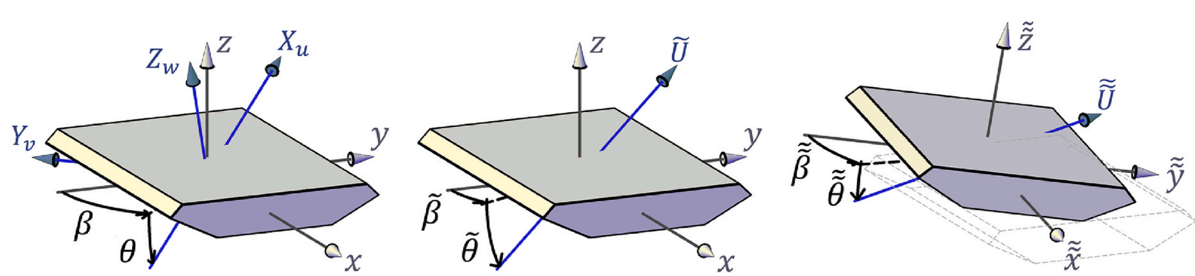

Fig. 3. Representation of global (mean) wind $Gw\ (X_u, Y_v, Z_w)$, local (static) structural $Ls\ (x,y,z)$ and local dynamic structural $\tilde{\tilde{Ls}}\ (\tilde{\tilde{x}},\tilde{\tilde{y}},\tilde{\tilde{z}})$ coordinate systems, local instantaneous wind speed $\tilde{U}$ (in the $X_{\tilde{U}}$-axis), local instantaneous relative wind speed $\tilde{\tilde{U}}$ (in the $X_{\tilde{\tilde{U}}}$-axis), and the pairs of angles (β,θ), $(\tilde{\beta},\tilde{\theta})$ and $(\tilde{\tilde{\beta}},\tilde{\tilde{\theta}})$.

$$\tilde{\theta} = \theta + \widetilde{\Delta\theta} \approx \theta + \frac{w}{U} \tag{42}$$

$$\boldsymbol{T}_{Gw\tilde{L}w} \approx \begin{bmatrix} 1 & -v/U & -w/U \\ v/U & 1 & -v\tan(\theta)/U \\ w/U & v\tan(\theta)/U & 1 \end{bmatrix} = \begin{bmatrix} 1 & -\widetilde{\Delta\beta}\cos\theta & -\widetilde{\Delta\theta} \\ \widetilde{\Delta\beta}\cos\theta & 1 & -\widetilde{\Delta\beta}\sin\theta \\ \widetilde{\Delta\theta} & \widetilde{\Delta\beta}\sin\theta & 1 \end{bmatrix} \tag{43}$$

$$\tilde{U}^2 \approx U^2 + 2Uu \tag{44}$$

The instantaneous aerodynamic coefficients can be also linearized with respect to the small angle variations $\widetilde{\Delta\beta}$ and $\widetilde{\Delta\theta}$, as in eq. (45).

$$\tilde{\boldsymbol{C}}_{\tilde{L}w} \approx \boldsymbol{C}_{Gw} + \boldsymbol{C}^{\prime\beta}_{Gw}\widetilde{\Delta\beta} + \boldsymbol{C}^{\prime\theta}_{Gw}\widetilde{\Delta\theta} \tag{45}$$

Where, for simplicity, $\tilde{\boldsymbol{C}} = \tilde{\boldsymbol{C}}(\tilde{\beta}, \tilde{\theta})$, $\boldsymbol{C} = \boldsymbol{C}(\beta, \theta)$, $\boldsymbol{C}^{\prime\beta} = \frac{\partial \boldsymbol{C}(\beta,\theta)}{\partial\beta}$ and $\boldsymbol{C}^{\prime\theta} = \frac{\partial \boldsymbol{C}(\beta,\theta)}{\partial\theta}$.

When the aerodynamic coefficients $\boldsymbol{C}$ are known for one system, e.g. Gw, they can be converted to another, e.g. Ls, through eq. (46). By partially differentiating both sides of eq. (46), $\boldsymbol{C}^{\prime\beta}$ and $\boldsymbol{C}^{\prime\theta}$ can be obtained as in eqs. (47) and (48).

$$\boldsymbol{C}_{Ls} = \boldsymbol{T}_{LsGw}\boldsymbol{C}_{Gw} \tag{46}$$

$$\boldsymbol{C}^{\prime\beta}_{Ls} = \frac{\partial(\boldsymbol{T}_{LsGw}\boldsymbol{C}_{Gw})}{\partial\beta} = \frac{\partial\boldsymbol{T}_{LsGw}}{\partial\beta}\boldsymbol{C}_{Gw} + \boldsymbol{T}_{LsGw}\boldsymbol{C}^{\prime\beta}_{Gw} \tag{47}$$

$$\boldsymbol{C}^{\prime\theta}_{Ls} = \frac{\partial(\boldsymbol{T}_{LsGw}\boldsymbol{C}_{Gw})}{\partial\theta} = \frac{\partial\boldsymbol{T}_{LsGw}}{\partial\theta}\boldsymbol{C}_{Gw} + \boldsymbol{T}_{LsGw}\boldsymbol{C}^{\prime\theta}_{Gw} \tag{48}$$

Finally, by linearizing the vector of the six buffeting forces per unit length $\tilde{\boldsymbol{f}}_{b,Gw}$, described in eqs. (39) and (35), and by combining eqs. (41)–(45), the buffeting forces can be approximated by eqs. (49)–(51), as a linear function of the turbulence components vector $\boldsymbol{a}_{Gw}$.

$$\tilde{\boldsymbol{f}}_{b,Gw} \approx \boldsymbol{A}_{b,Gw}\,\boldsymbol{a}_{Gw} \tag{49}$$

$$\boldsymbol{a}_{Gw} = [u, v, w]^T \tag{50}$$

$$\boldsymbol{A}_{b,Gw} = \frac{1}{2}\rho U \begin{bmatrix} 2BC_{X_u}\chi_{X_u,u} & B\left(C^{\prime\beta}_{X_u}/\cos\theta - C_{Y_v}\right)\chi_{X_u,v} & B\left(C^{\prime\theta}_{X_u} - C_{Z_w}\right)\chi_{X_u,w} \\ 2BC_{Y_v}\chi_{Y_v,u} & B\left(C_{X_u} + C^{\prime\beta}_{Y_v}/\cos\theta - C_{Z_w}\tan\theta\right)\chi_{Y_v,v} & BC^{\prime\theta}_{Y_v}\chi_{Y_v,w} \\ 2BC_{Z_w}\chi_{Z_w,u} & B\left(C_{Y_v}\tan\theta + C^{\prime\beta}_{Z_w}/\cos\theta\right)\chi_{Z_w,v} & B\left(C_{X_u} + C^{\prime\theta}_{Z_w}\right)\chi_{Z_w,w} \\ 2B^2C_{rX_u}\chi_{rX_u,u} & B^2\left(C^{\prime\beta}_{rX_u}/\cos\theta - C_{rY_v}\right)\chi_{rX_u,v} & B^2\left(C^{\prime\theta}_{rX_u} - C_{rZ_w}\right)\chi_{rX_u,w} \\ 2B^2C_{rY_v}\chi_{rY_v,u} & B^2\left(C_{rX_u} + C^{\prime\beta}_{rY_v}/\cos\theta - C_{rZ_w}\tan\theta\right)\chi_{rY_v,v} & B^2C^{\prime\theta}_{rY_v}\chi_{rY_v,w} \\ 2B^2C_{rZ_w}\chi_{rZ_w,u} & B^2\left(C_{rY_v}\tan\theta + C^{\prime\beta}_{rZ_w}/\cos\theta\right)\chi_{rZ_w,v} & B^2\left(C_{rX_u} + C^{\prime\theta}_{rZ_w}\right)\chi_{rZ_w,w} \end{bmatrix} \tag{51}$$

Where the function $\chi_{i,j}$, the so-called cross-sectional admittance function, associated with the aerodynamic coefficient C_i and the turbulence component j, is introduced to reflect the sensitivity of the cross-section to different frequency components.

3.2. Fluctuating wind forces due to turbulence and structural motions

3.2.1. Non-linear forces

The wind action is represented, at each time instant, by a relative wind speed $\tilde{\tilde{U}}$, and the instantaneous motion-dependent yaw and inclination angles $\tilde{\tilde{\beta}}$ and $\tilde{\tilde{\theta}}$. When the wind moves a bridge element, its displaced local axes compose the $\tilde{\tilde{L}}s$ system, as illustrated in Fig. 3. These motion-dependent variables help define the instantaneous vector of motion-dependent aerodynamic forces in eqs. (52)–(54).

$$\tilde{\tilde{\boldsymbol{f}}}_{ad,Gw} = \boldsymbol{T}_{Gw\tilde{\tilde{L}}w}\, 1/2\,\rho\,\tilde{\tilde{U}}^2\,\boldsymbol{B}\,\tilde{\tilde{\boldsymbol{C}}}_{\tilde{\tilde{L}}w} \tag{52}$$

$$\boldsymbol{T}_{Gw\tilde{\tilde{L}}w} = \boldsymbol{T}_{GwLs}\,\boldsymbol{T}_{Ls\tilde{\tilde{L}}s}\,\boldsymbol{T}_{\tilde{\tilde{L}}s\tilde{\tilde{L}}w} \tag{53}$$

$$\boldsymbol{T}_{\tilde{\tilde{L}}s\tilde{\tilde{L}}w} = (\boldsymbol{R}_Y(\tilde{\tilde{\theta}})\boldsymbol{R}_Z(-\tilde{\tilde{\beta}} - \pi/2)\,)^T \tag{54}$$

$\tilde{\tilde{U}}$ is defined in eq. (25), $\boldsymbol{T}_{Ls\tilde{\tilde{L}}s}$ can be obtained through eq. (2) or approximated by eq. (28) or by eq. (29), and $\tilde{\tilde{\boldsymbol{C}}}_{\tilde{\tilde{L}}w}(\tilde{\tilde{\beta}}, \tilde{\tilde{\theta}})$ is a function of the angles $\tilde{\tilde{\beta}}$ and $\tilde{\tilde{\theta}}$, both defined in eqs. (30) and (31).

3.2.2. Linearizations

The linearization process described in section 3.1.2, with respect to u, v and w, can be expanded to include linearizations of the structural angular displacements and the structural translation velocities. The structural angular displacements are included in Δ and can be assumed to follow the small angle approximation, whereas the structural translational velocities are included in $\dot{\Delta}$ and can be assumed small, relatively to the mean wind speed U. These assumptions allow eqs. (30) and (31) to be linearized into eqs. (55) and (56). These expressions are most compact when the structural motions, Δ_{Gw} and $\dot{\Delta}_{Gw}$, are represented in the Gw system. Similarly, $\boldsymbol{T}_{Gw\tilde{\tilde{L}}w}$ and $\tilde{\tilde{U}}^2$ are linearized into eqs. (57) and (58).

$$\tilde{\tilde{\beta}} = \beta + \widetilde{\widetilde{\Delta\beta}} \approx \beta + \frac{\tilde{\tilde{v}}}{U\cos\theta} - \frac{\Delta_{rZ_w}}{\cos\theta} \tag{55}$$

$$\tilde{\tilde{\theta}} = \theta + \widetilde{\widetilde{\Delta\theta}} \approx \theta + \frac{\tilde{\tilde{w}}}{U} + \Delta_{rY_v} \tag{56}$$

$$\boldsymbol{T}_{Gw\tilde{\tilde{L}}w} \approx \begin{bmatrix} 1 & -\tilde{\tilde{v}}/U & -\tilde{\tilde{w}}/U \\ \tilde{\tilde{v}}/U & 1 & -\Delta_{rX_u} + (\Delta_{rZ_w} - \tilde{\tilde{v}}/U)\tan(\theta) \\ \tilde{\tilde{w}}/U & \Delta_{rX_u} + (\tilde{\tilde{v}}/U - \Delta_{rZ_w})\tan(\theta) & 1 \end{bmatrix} \tag{57}$$

$$\tilde{\tilde{U}}^2 \approx U^2 + 2U\tilde{\tilde{u}} \tag{58}$$

Where $[\Delta_{rX_u}, \Delta_{rY_v}, \Delta_{rZ_w}]^T = \boldsymbol{T}_{GwLs}[\Delta_{rx}, \Delta_{ry}, \Delta_{rz}]^T$.

Again, by linearizing $\tilde{\tilde{\boldsymbol{C}}}_{\tilde{\tilde{L}}w} \approx \boldsymbol{C}_{Gw} + \boldsymbol{C}^{\prime\beta}_{Gw}\widetilde{\widetilde{\Delta\beta}} + \boldsymbol{C}^{\prime\theta}_{Gw}\widetilde{\widetilde{\Delta\theta}}$, combining eqs.

(55)–(58) and linearizing the vector of the six buffeting forces per unit length $\widetilde{\widetilde{\boldsymbol{f}}}_{\boldsymbol{b},\boldsymbol{Gw}}=\widetilde{\widetilde{\boldsymbol{f}}}_{\boldsymbol{ad},\boldsymbol{Gw}}-\boldsymbol{f}_{\boldsymbol{mean},\boldsymbol{Gw}}$ (see eqs. (52) and (39)), $\widetilde{\widetilde{\boldsymbol{f}}}_{\boldsymbol{b},\boldsymbol{Gw}}$ can be approximated by eqs. (59)–(64), as a linear function of the turbulence components, the structural displacements and the structural velocities.

$$\widetilde{\widetilde{\boldsymbol{f}}}_{\boldsymbol{b},\boldsymbol{Gw}}\approx\widetilde{\boldsymbol{f}}_{\boldsymbol{b},\boldsymbol{Gw}}+\boldsymbol{A}_{\Delta,\boldsymbol{Gw}}\ \boldsymbol{\Delta}_{\boldsymbol{Gw}}+\boldsymbol{A}_{\dot{\Delta},\boldsymbol{Gw}}\ \dot{\boldsymbol{\Delta}}_{\boldsymbol{Gw}} \tag{59}$$

$$\boldsymbol{\Delta}_{\boldsymbol{Gw}}=[\Delta_{X_u},\Delta_{Y_v},\Delta_{Z_w},\Delta_{rX_u},\Delta_{rY_v},\Delta_{rZ_w}]^T \tag{60}$$

$$\dot{\boldsymbol{\Delta}}_{\boldsymbol{Gw}}=[\dot{\Delta}_{X_u},\dot{\Delta}_{Y_v},\dot{\Delta}_{Z_w},\dot{\Delta}_{rX_u},\dot{\Delta}_{rY_v},\dot{\Delta}_{rZ_w}]^T \tag{61}$$

$$\boldsymbol{A}_{\Delta,\boldsymbol{Gw}}=\left[\boldsymbol{0}\ \ \boldsymbol{0}\ \ \boldsymbol{0}\ \ \boldsymbol{A}_{\Delta_{rX_u}}\ \ \boldsymbol{A}_{\Delta_{rY_v}}\ \ \boldsymbol{A}_{\Delta_{rZ_w}}\right]$$
$$=\frac{1}{2}\rho U^2\begin{bmatrix} 0\ 0\ 0\ 0 & BC'^{\theta}_{X_u} & -BC'^{\beta}_{X_u}/\cos\theta \\ 0\ 0\ 0\ -BC_{Z_w} & BC'^{\theta}_{Y_v} & -B\left(C'^{\beta}_{Y_v}-C_{Z_w}\sin\theta\right)/\cos\theta \\ 0\ 0\ 0\ BC_{Y_v} & BC'^{\theta}_{Z_w} & -B\left(C'^{\beta}_{Z_w}+C_{Y_v}\sin\theta\right)/\cos\theta \\ 0\ 0\ 0\ 0 & B^2C'^{\theta}_{rX_u} & -B^2C'^{\beta}_{rX_u}/\cos\theta \\ 0\ 0\ 0\ -B^2C_{rZ_w} & B^2C'^{\theta}_{rY_v} & -B^2\left(C'^{\beta}_{rY_v}-C_{rZ_w}\sin\theta\right)/\cos\theta \\ 0\ 0\ 0\ B^2C_{rY_v} & B^2C'^{\theta}_{rZ_w} & -B^2\left(C'^{\beta}_{rZ_w}+C_{rY_v}\sin\theta\right)/\cos\theta \end{bmatrix} \tag{62}$$

$$P_1^*=1\Big/k\Big(C_{X_u}\left(-\cos^2\beta\cos^2\theta-1\right)+C_{Y_v}\left(2\cos^2\theta-1\right)\sin\beta\cos\beta\Big/\cos\theta+C_{Z_w}\left(1-\sin^2\theta\cos^2\beta\right)\tan\theta+C'^{\beta}_{X_u}\sin\beta\cos\beta-C'^{\beta}_{Y_v}\sin^2\beta\Big/\cos\theta$$
$$-C'^{\beta}_{Z_w}\sin\beta\cos\beta\tan\theta+C'^{\theta}_{X_u}\sin\theta\cos^2\beta\cos\theta-C'^{\theta}_{Y_v}\sin\beta\sin\theta\cos\beta-C'^{\theta}_{Z_w}\sin^2\theta\cos^2\beta\Big) \tag{70}$$

$$\boldsymbol{A}_{\dot{\Delta},\boldsymbol{Gw}}=\left[\boldsymbol{A}_{\dot{\Delta}_{X_u}}\ \ \boldsymbol{A}_{\dot{\Delta}_{Y_v}}\ \ \boldsymbol{A}_{\dot{\Delta}_{Z_w}}\ \ \boldsymbol{0}\ \ \boldsymbol{0}\ \ \boldsymbol{0}\right] \tag{63}$$

$$\left[\boldsymbol{A}_{\dot{\Delta}_{X_u}}\ \ \boldsymbol{A}_{\dot{\Delta}_{Y_v}}\ \ \boldsymbol{A}_{\dot{\Delta}_{Z_w}}\right]=-\boldsymbol{A}_{\boldsymbol{b},\boldsymbol{Gw}}\left(\chi_{i,j}=1\right) \tag{64}$$

Where $\widetilde{\boldsymbol{f}}_{\boldsymbol{b},\boldsymbol{Gw}}$ is described and linearized in section 3.1, $\boldsymbol{0}=[0,0,0,0,0,0]^T$ and where $\boldsymbol{A}_{\boldsymbol{b},\boldsymbol{Gw}}(\chi_{i,j}=1)$ is found in eq. (51), for all $\chi_{i,j}=1$.

Another common alternative is to formulate the motion-dependent forces using Scanlan's flutter derivatives (Scanlan and Tomo, 1971), as shown in eqs. (65)–(69), in the *Ls* system. These frequency-dependent flutter derivatives can be obtained experimentally, as done in e.g. (Zhu et al., 2002a).

$$\widetilde{\widetilde{\boldsymbol{f}}}_{\boldsymbol{b},\boldsymbol{Ls}}\approx\widetilde{\boldsymbol{f}}_{\boldsymbol{b},\boldsymbol{Ls}}+\boldsymbol{A}_{\Delta,\boldsymbol{Ls}}\ \boldsymbol{\Delta}_{\boldsymbol{Ls}}+\boldsymbol{A}_{\dot{\Delta},\boldsymbol{Ls}}\ \dot{\boldsymbol{\Delta}}_{\boldsymbol{Ls}} \tag{65}$$

$$\boldsymbol{\Delta}_{\boldsymbol{Ls}}=\left[\Delta_x,\Delta_y,\Delta_z,\Delta_{rx},\Delta_{ry},\Delta_{rz}\right]^T \tag{66}$$

$$\dot{\boldsymbol{\Delta}}_{\boldsymbol{Ls}}=\left[\dot{\Delta}_x,\dot{\Delta}_y,\dot{\Delta}_z,\dot{\Delta}_{rx},\dot{\Delta}_{ry},\dot{\Delta}_{rz}\right]^T \tag{67}$$

$$\boldsymbol{A}_{\boldsymbol{Scanlan},\Delta,\boldsymbol{Ls}}=\frac{1}{2}\rho U^2k^2\begin{bmatrix} 0 & 0 & 0 & 0 & 0 & 0 \\ 0 & P_4^* & P_6^* & BP_3^* & 0 & 0 \\ 0 & H_6^* & H_4^* & BH_3^* & 0 & 0 \\ 0 & BA_6^* & BA_4^* & B^2A_3^* & 0 & 0 \\ 0 & 0 & 0 & 0 & 0 & 0 \\ 0 & 0 & 0 & 0 & 0 & 0 \end{bmatrix} \tag{68}$$

$$\boldsymbol{A}_{\boldsymbol{Scanlan},\dot{\Delta},\boldsymbol{Ls}}=\frac{1}{2}\rho Uk\begin{bmatrix} 0 & 0 & 0 & 0 & 0 & 0 \\ 0 & BP_1^* & BP_5^* & B^2P_2^* & 0 & 0 \\ 0 & BH_5^* & BH_1^* & B^2H_2^* & 0 & 0 \\ 0 & B^2A_5^* & B^2A_1^* & B^3A_2^* & 0 & 0 \\ 0 & 0 & 0 & 0 & 0 & 0 \\ 0 & 0 & 0 & 0 & 0 & 0 \end{bmatrix} \tag{69}$$

Here $k=B\omega/U$ is the reduced frequency. In the absence of such experimental results it is possible to compare Scanlan's expressions with the previously derived expressions for $\boldsymbol{A}_{\Delta}$ and $\boldsymbol{A}_{\dot{\Delta}}$, in the same coordinate system (e.g. through $\boldsymbol{A}_{\boldsymbol{Scanlan},\Delta,\boldsymbol{Ls}}=\boldsymbol{T}_{\boldsymbol{LsGw}}\boldsymbol{A}_{\Delta,\boldsymbol{Gw}}\boldsymbol{T}_{\boldsymbol{GwLs}}$ and $\boldsymbol{A}_{\boldsymbol{Scanlan},\dot{\Delta},\boldsymbol{Ls}}=\boldsymbol{T}_{\boldsymbol{LsGw}}\boldsymbol{A}_{\dot{\Delta},\boldsymbol{Gw}}\boldsymbol{T}_{\boldsymbol{GwLs}}$), rendering the quasi-static flutter derivatives in eqs. (70)–(78).

$$P_3^*=1\Big/k^2\Big(C_{Y_v}\sin\beta\cos\beta\tan\theta-C_{Z_w}\sin^2\beta\Big/\cos\theta-C'^{\beta}_{X_u}\sin\beta\sin\theta\cos\beta$$
$$+C'^{\beta}_{Y_v}\sin^2\beta\tan\theta+C'^{\beta}_{Z_w}\sin\beta\sin\theta\cos\beta\tan\theta-C'^{\theta}_{X_u}\cos^2\beta\cos\theta$$
$$+C'^{\theta}_{Y_v}\sin\beta\cos\beta+C'^{\theta}_{Z_w}\sin\theta\cos^2\beta\Big) \tag{71}$$

$$P_5^*=1\Big/k\Big(-C_{X_u}\sin\theta\cos\beta\cos\theta+2C_{Y_v}\sin\beta\sin\theta+C_{Z_w}\left(\sin^2\theta+1\right)\cos\beta$$
$$-C'^{\theta}_{X_u}\cos\beta\cos^2\theta+C'^{\theta}_{Y_v}\sin\beta\cos\theta+C'^{\theta}_{Z_w}\sin\theta\cos\beta\cos\theta\Big) \tag{72}$$

$$H_1^*=1\Big/k\Big(C_{X_u}\left(\cos^2\theta-2\right)-C_{Z_w}\sin\theta\cos\theta-C'^{\theta}_{X_u}\sin\theta\cos\theta-C'^{\theta}_{Z_w}\cos^2\theta\Big) \tag{73}$$

$$H_3^*=1\Big/k^2\Big(-C_{Y_v}\sin\beta-C'^{\beta}_{X_u}\sin\beta\sin\theta\tan\theta-C'^{\beta}_{Z_w}\sin\beta\sin\theta$$
$$-C'^{\theta}_{X_u}\sin\theta\cos\beta-C'^{\theta}_{Z_w}\cos\beta\cos\theta\Big) \tag{74}$$

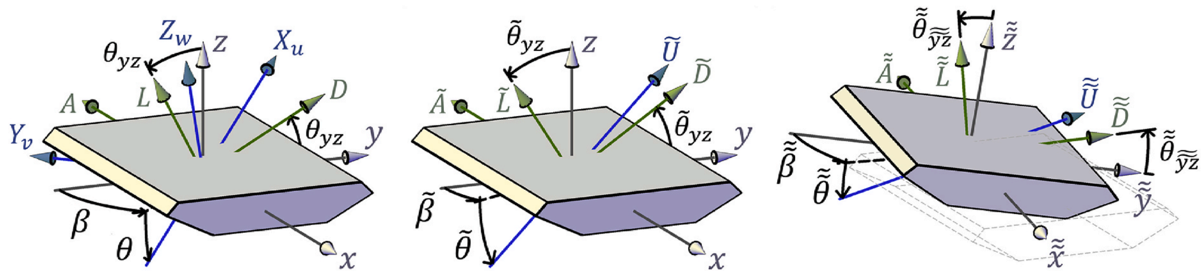

Fig. 4. Representation of Gw (X_u,Y_v,Z_w), Ls (x,y,z), $\widetilde{\widetilde{Ls}}$ $(\tilde{\tilde{x}},\tilde{\tilde{y}},\tilde{\tilde{z}})$, $\tilde{U}$, $\tilde{\tilde{U}}$, (β,θ), $(\tilde{\beta},\tilde{\theta})$, $(\tilde{\tilde{\beta}},\tilde{\tilde{\theta}})$ and the newly defined angles θ_{yz}, $\tilde{\theta}_{yz}$ and $\tilde{\tilde{\theta}}_{\tilde{\tilde{yz}}}$ and systems Lnw (D,A,L), $\widetilde{Lnw}$ $(\tilde{D},\tilde{A},\tilde{L})$ and $\widetilde{\widetilde{Lnw}}$ $(\tilde{\tilde{D}},\tilde{\tilde{A}},\tilde{\tilde{L}})$.

$$H_5^* = 1\Big/k\Big(-C_{X_u}\sin\theta\cos\beta\cos\theta + C_{Z_w}\left(\sin^2\theta-2\right)\cos\beta + C_{X_u}^{\prime\beta}\sin\beta\tan\theta + C_{Z_w}^{\prime\beta}\sin\beta + C_{X_u}^{\prime\theta}\sin^2\theta\cos\beta + C_{Z_w}^{\prime\theta}\sin\theta\cos\beta\cos\theta\Big) \quad (75)$$

$$A_1^* = 1\Big/k\Big(C_{rX_u}\sin\beta\sin\theta\cos\theta + 2C_{rY_v}\sin\theta\cos\beta + C_{rZ_w}\left(\cos^2\theta-2\right)\sin\beta + C_{rX_u}^{\prime\theta}\sin\beta\cos^2\theta + C_{rY_v}^{\prime\theta}\cos\beta\cos\theta - C_{rZ_w}^{\prime\theta}\sin\beta\sin\theta\cos\theta\Big) \quad (76)$$

$$A_3^* = 1\Big/k^2\Big(-C_{rY_v}\sin^2\beta\tan\theta - C_{rZ_w}\sin\beta\cos\beta\Big/\cos\theta + C_{rX_u}^{\prime\beta}\sin^2\beta\sin\theta + C_{rY_v}^{\prime\beta}\sin\beta\cos\beta\tan\theta - C_{rZ_w}^{\prime\beta}\sin^2\beta\sin\theta\tan\theta + C_{rX_u}^{\prime\theta}\sin\beta\cos\beta\cos\theta + C_{rY_v}^{\prime\theta}\cos^2\beta - C_{rZ_w}^{\prime\theta}\sin\beta\sin\theta\cos\beta\Big) \quad (77)$$

$$A_5^* = 1\Big/k\Big(C_{rX_u}\sin\beta\cos\beta\cos^2\theta + C_{rY_v}\left(\sin^2\beta\big/\cos\theta + 2\cos^2\beta\cos\theta\right) + C_{rZ_w}\sin\beta\sin^2\theta\cos\beta\tan\theta - C_{rX_u}^{\prime\beta}\sin^2\beta - C_{rY_v}^{\prime\beta}\sin\beta\cos\beta\Big/\cos\theta + C_{rZ_w}^{\prime\beta}\sin^2\beta\tan\theta - C_{rX_u}^{\prime\theta}\sin\beta\sin\theta\cos\beta\cos\theta - C_{rY_v}^{\prime\theta}\sin\theta\cos^2\beta + C_{rZ_w}^{\prime\theta}\sin\beta\sin^2\theta\cos\beta\Big) \quad (78)$$

The reduced frequency k cancels out when substituting these quasi-static flutter derivatives in Scanlan's expressions. The remaining flutter derivatives P_i^*, H_i^* and A_i^*, for $i = 2, 4, 6$, are equal to zero.

It should be noted that Scanlan's flutter derivatives were developed for mean winds normal to the bridge girder. These typically consider only 3 DOF, namely $\dot{\Delta}_y, \dot{\Delta}_z$ and Δ_{rx}, and could thus be incomplete for skew wind analyses.

4. A 2D (+1D) buffeting approach for skew winds

A 3D buffeting approach (section 3) should be preferred when possible. It has been observed that buffeting responses vary with β and θ in a way that resembles the same variation of the corresponding aerodynamic coefficients $\boldsymbol{C}(\beta,\theta)$ with β and θ (Zhu, 2002). However, this information is not always available and wind tunnel tests and CFD analyses are commonly only performed for wind normal to the bridge girder, limiting the available information to $\boldsymbol{C}(\beta=0,\theta)$. For preliminary assessments and comparison purposes, a novel generalization of the 2D normal projection concept is presented, for any β and θ. The (+1D) signature alludes to the option of including the contribution from the axial loads in the longitudinal dimension when an axial force coefficient is available.

The approach presented in this section assumes the validity of decomposing the three-dimensional wind-structure interaction into two independent problems:

1. A two-dimensional wind-structure interaction in the normal plane, where the relevant wind components are those projected onto either the static $\boldsymbol{yz}$-plane or the moving $\tilde{\tilde{\boldsymbol{y}}}\tilde{\tilde{\boldsymbol{z}}}$-plane. The aerodynamic coefficients (drag, lift and moment) are only dependent on the normal projections of the inclination angles θ_{yz}, $\tilde{\theta}_{yz}$ and $\tilde{\tilde{\theta}}_{\tilde{\tilde{yz}}}$, also called angles-of-attack.
2. A one-dimensional wind-structure interaction in the longitudinal static $\boldsymbol{x}$- or dynamic $\tilde{\tilde{\boldsymbol{x}}}$-axis to account for the axial forces (due to e.g. drag forces on railings, bridge equipment, vehicles, other transversal elements, as well as viscous forces along all exposed surfaces).

The present approach is a generalization of the so-called *cosine rule* and *sine rule*, from the domain in which they were derived (for $\theta = 0$), to the more general case of arbitrary values of β and θ. It also expands the motion-dependencies from 3 DOF ($\boldsymbol{y}$, $\boldsymbol{z}$ and $\boldsymbol{rx}$), to all 6 DOF (e.g. for $\beta = 45°$, a small positive Δ_{rz} will make the bridge more normal to the wind, increasing the normal wind speed and associated forces).

4.1. The local normal wind coordinate systems and associated variables

The mean wind speed projection onto the $\boldsymbol{yz}$-plane, U_{yz}, and its mean angle-of-attack θ_{yz}, as well as their instantaneous (turbulence-dependent) and instantaneous relative (turbulence- and motion-dependent) counterparts are described in eqs. (79)–(84).

Normal wind quantities:			
$U_{yz} = \sqrt{U_y^2 + U_z^2}$	(79)	$\theta_{yz} = \arcsin(U_z/U_{yz})$	(80)
$\tilde{U}_{yz} = \sqrt{\tilde{U}_y^2 + \tilde{U}_z^2}$	(81)	$\tilde{\theta}_{yz} = \arcsin(\tilde{U}_z/\tilde{U}_{yz})$	(82)
$\tilde{\tilde{U}}_{\tilde{\tilde{yz}}} = \sqrt{\tilde{\tilde{U}}_{\tilde{\tilde{y}}}^2 + \tilde{\tilde{U}}_{\tilde{\tilde{z}}}^2}$	(83)	$\tilde{\tilde{\theta}}_{\tilde{\tilde{yz}}} = \arcsin(\tilde{\tilde{U}}_{\tilde{\tilde{z}}}/\tilde{\tilde{U}}_{\tilde{\tilde{yz}}})$	(84)

Three additional right-handed orthogonal coordinate systems are adopted, namely the local (mean) normal wind Lnw $(\boldsymbol{D},\boldsymbol{A},\boldsymbol{L})$ the local instantaneous normal wind $\widetilde{Lnw}$ $(\tilde{\boldsymbol{D}},\tilde{\boldsymbol{A}},\tilde{\boldsymbol{L}})$ and the local relative instantaneous normal wind $\widetilde{\widetilde{Lnw}}$ $(\tilde{\tilde{\boldsymbol{D}}},\tilde{\tilde{\boldsymbol{A}}},\tilde{\tilde{\boldsymbol{L}}})$. The axes $\boldsymbol{D}$, $\boldsymbol{A}$ and $\boldsymbol{L}$ refer to the drag, axial and lift directions. $\boldsymbol{D}$, $\tilde{\boldsymbol{D}}$ and $\tilde{\tilde{\boldsymbol{D}}}$ describe the direction of the projected wind speeds U_{yz}, $\tilde{U}_{yz}$ and $\tilde{\tilde{U}}_{\tilde{\tilde{yz}}}$, respectively. In a 6 DOF representation of the local normal wind coordinate system, Lnw $(\boldsymbol{D},\boldsymbol{A},\boldsymbol{L},\boldsymbol{rD},\boldsymbol{M},\boldsymbol{rL})$, the axis $\boldsymbol{M}$ represents the moment, as a rotation about the $\boldsymbol{A}$ axis. These coordinate systems are defined in eqs. (85)–(88) and illustrated in Fig. 4, together with the newly defined variables from eqs. (79)–(84).

$$\boldsymbol{D} = \left(U_y\boldsymbol{y} + U_z\boldsymbol{z}\right)\big/U_{yz};\quad \boldsymbol{A} = -\boldsymbol{x}\cdot S;\quad \boldsymbol{L} = \boldsymbol{D}\times\boldsymbol{A} \quad (85)$$

$$\tilde{\boldsymbol{D}} = \left(\tilde{U}_y\boldsymbol{y} + \tilde{U}_z\boldsymbol{z}\right)\big/\tilde{U}_{yz};\quad \tilde{\boldsymbol{A}} = -\boldsymbol{x}\cdot\tilde{S};\quad \tilde{\boldsymbol{L}} = \tilde{\boldsymbol{D}}\times\tilde{\boldsymbol{A}} \quad (86)$$

$$\tilde{\tilde{\boldsymbol{D}}} = \left(\tilde{\tilde{U}}_{\tilde{\tilde{y}}}\tilde{\tilde{\boldsymbol{y}}} + \tilde{\tilde{U}}_{\tilde{\tilde{z}}}\tilde{\tilde{\boldsymbol{z}}}\right)\big/\tilde{\tilde{U}}_{\tilde{\tilde{yz}}};\quad \tilde{\tilde{\boldsymbol{A}}} = -\tilde{\tilde{\boldsymbol{x}}}\cdot\tilde{\tilde{S}};\quad \tilde{\tilde{\boldsymbol{L}}} = \tilde{\tilde{\boldsymbol{D}}}\times\tilde{\tilde{\boldsymbol{A}}} \quad (87)$$

$$S = sgn(\cos\beta);\quad \tilde{S} = sgn(\cos\tilde{\beta});\quad \tilde{\tilde{S}} = sgn(\cos\tilde{\tilde{\beta}}) \quad (88)$$

The transformation matrices between Lnw, $\widetilde{Lnw}$, $\widetilde{\widetilde{Lnw}}$ and the previously defined Ls and $\widetilde{\widetilde{Ls}}$ systems can be obtained, for instance, as in eqs. (89)–(91).

$$\boldsymbol{T}_{\boldsymbol{LsLnw}} = \left(\boldsymbol{R}_Y\left(\theta_{yz}\right)\,\boldsymbol{R}_Z(-S\,\pi/2)\right)^T \tag{89}$$

$$\boldsymbol{T}_{\boldsymbol{Ls}\widetilde{\boldsymbol{Lnw}}} = \left(\boldsymbol{R}_Y\left(\widetilde{\theta}_{yz}\right)\,\boldsymbol{R}_Z(-\widetilde{S}\,\pi/2)\right)^T \tag{90}$$

$$\boldsymbol{T}_{\widetilde{\widetilde{\boldsymbol{Ls}}}\widetilde{\widetilde{\boldsymbol{Lnw}}}} = \left(\boldsymbol{R}_Y(\widetilde{\widetilde{\theta}}_{\widetilde{yz}})\,\boldsymbol{R}_Z(-\widetilde{\widetilde{S}}\,\pi/2)\right)^T \tag{91}$$

Finally, it can be convenient to express the turbulence components in the Lnw system as a function of the original components in the Gw system (see eq. (92)).

$$\boldsymbol{a}_{\boldsymbol{Lnw}} = [a_D, a_A, a_L]^T = \boldsymbol{T}_{\boldsymbol{LnwGw}}\,\boldsymbol{a}_{\boldsymbol{Gw}} = \boldsymbol{T}^T_{\boldsymbol{LsLnw}}\,\boldsymbol{T}_{\boldsymbol{LsGw}}\,[u, v, w]^T \tag{92}$$

4.2. Fluctuating wind forces due to turbulence

4.2.1. Non-linear forces

The vector of six aerodynamic forces $\widetilde{\boldsymbol{F}}_{\boldsymbol{ad,Gs}}$ in the Gs system, for each bridge element, can be obtained from eqs. (93) and (94).

$$\widetilde{\boldsymbol{F}}_{\boldsymbol{ad,Gs}} = L\,\boldsymbol{T}_{\boldsymbol{GsLs}}\,\boldsymbol{T}_{\boldsymbol{LsLnw}}\,\widetilde{\boldsymbol{f}}_{\boldsymbol{ad,Lnw}} \tag{93}$$

$$\widetilde{\boldsymbol{f}}_{\boldsymbol{ad,Lnw}} = \boldsymbol{T}_{\boldsymbol{Lnw}\widetilde{\boldsymbol{Lnw}}}\,1\big/2\,\rho\,\widetilde{U}^2_{yz}\boldsymbol{B}_{\boldsymbol{Lnw}}\widetilde{\boldsymbol{C}}_{\widetilde{\boldsymbol{Lnw}}} \tag{94}$$

Where $\boldsymbol{B}_{\boldsymbol{Lnw}} = diag(H, 0, B, 0, B^2, 0)$ is a diagonal matrix and H is the cross-section height as typically used to normalize C_D. $\widetilde{\boldsymbol{C}}_{\widetilde{\boldsymbol{Lnw}}}(\widetilde{\theta}_{yz}) = [\widetilde{C}_{\widetilde{D}}, 0, \widetilde{C}_{\widetilde{L}}, 0, \widetilde{C}_{\widetilde{M}}, 0]^T$ is the vector of aerodynamic coefficients in the $\widetilde{Lnw}$ system, for an instantaneous projected angle of attack $\widetilde{\theta}_{yz}$. $\boldsymbol{T}_{\boldsymbol{Lnw}\widetilde{\boldsymbol{Lnw}}} = \boldsymbol{T}_{\boldsymbol{LnwLs}}\boldsymbol{T}_{\boldsymbol{Ls}\widetilde{\boldsymbol{Lnw}}}$ is the transformation matrix from $\widetilde{Lnw}$ to Lnw.

The vector of normal wind buffeting forces per unit length and for each element, containing the time-varying drag, lift and moment forces, is given in eq. (95) by simply subtracting the mean normal wind forces $\boldsymbol{f}_{\boldsymbol{mean,Lnw}}$, where $\boldsymbol{C}_{\boldsymbol{Lnw}}(\theta_{yz}) = [C_D, 0, C_L, 0, C_M, 0]^T$.

$$\widetilde{\boldsymbol{f}}_{\boldsymbol{b,Lnw}} = \widetilde{\boldsymbol{f}}_{\boldsymbol{ad,Lnw}} - \boldsymbol{f}_{\boldsymbol{mean,Lnw}} = \widetilde{\boldsymbol{f}}_{\boldsymbol{ad,Lnw}} - 1\big/2\,\rho\,U^2_{yz}\boldsymbol{B}_{\boldsymbol{Lnw}}\boldsymbol{C}_{\boldsymbol{Lnw}} \tag{95}$$

4.2.2. Linearizations

The vector of buffeting forces $\widetilde{\boldsymbol{f}}_{\boldsymbol{b,Lnw}}$ is a non-linear function of the turbulence components, either represented as u, v and w, or as a_D, a_A and a_L. The linearization process conducted in section 3.1.2 can be repeated here.

Limitation: The linear approximations presented in this section should not be used whenever $\widetilde{U}_y$ oscillates between positive and negative values, i.e. in the vicinity of $\beta\ \sim \pm 90^\circ$. The functions $\boldsymbol{T}_{\boldsymbol{Ls}\widetilde{\boldsymbol{Lnw}}}$ and $\widetilde{\theta}_{yz}$ will have singularities at $\widetilde{\beta}\ = \pm\,90^\circ$ (Example: when β is close to 90° the $\boldsymbol{y}$-projected turbulence can be larger than the $\boldsymbol{y}$-projected mean wind, which can abruptly change the instantaneous drag direction $\widetilde{\boldsymbol{D}}$ at each time instant). It is thus assumed that $\widetilde{S} = S$ for all time steps.

By conveniently adopting a representation that uses a_D, a_A and a_L, instead of u, v and w, the linearization of $\widetilde{U}^2_{yz}$, $\widetilde{\theta}_{yz}$, $\boldsymbol{T}_{\boldsymbol{Lnw}\widetilde{\boldsymbol{Lnw}}}$ (assuming $S = \widetilde{S}$) and $\widetilde{\boldsymbol{C}}_{\widetilde{\boldsymbol{Lnw}}}$ follows in eqs. (96)–(99).

$$\widetilde{U}^2_{yz} \approx U^2_{yz} + 2U_{yz}a_D \tag{96}$$

$$\widetilde{\theta}_{yz} = \theta_{yz} + \widetilde{\Delta\theta}_{yz} \approx \theta_{yz} + \frac{a_L}{U_{yz}} \tag{97}$$

$$\boldsymbol{T}_{\boldsymbol{Lnw}\widetilde{\boldsymbol{Lnw}}}(\widetilde{S} = S) = \left(\boldsymbol{R}_Y\left(\widetilde{\theta}_{yz}\right)\,\boldsymbol{R}_Y\left(-\theta_{yz}\right)\right)^T \approx \begin{bmatrix} 1 & 0 & -\widetilde{\Delta\theta}_{yz} \\ 0 & 1 & 0 \\ \widetilde{\Delta\theta}_{yz} & 0 & 1 \end{bmatrix} \tag{98}$$

$$\widetilde{\boldsymbol{C}}_{\widetilde{\boldsymbol{Lnw}}} \approx \boldsymbol{C}_{\boldsymbol{Lnw}} + \boldsymbol{C}'_{\boldsymbol{Lnw}}\,\widetilde{\Delta\theta}_{yz} \tag{99}$$

Where $\boldsymbol{C}'_{\boldsymbol{Lnw}} = \frac{\partial C_{Lnw}(\theta_{yz})}{\partial\theta_{yz}} = [C'_D, 0, C'_L, 0, C'_M, 0]^T$ is the vector of aerodynamic coefficient derivatives with respect to the angle-of-attack, at a mean angle θ_{yz}.

The vector of linearized normal buffeting forces due to the $\boldsymbol{yz}$-projected wind, $\widetilde{\boldsymbol{f}}_{\boldsymbol{b,Lnw}}$, after being linearized with respect to the turbulence components, can be then separated into a coefficient matrix $\boldsymbol{A}_{\boldsymbol{b,Lnw}}$ and the turbulence components vector $\boldsymbol{a}_{\boldsymbol{Lnw}} = [a_D, a_A, a_L]^T$, as in eqs. (100) and (101).

$$\widetilde{\boldsymbol{f}}_{\boldsymbol{b,Lnw}} \approx \boldsymbol{A}_{\boldsymbol{b,Lnw}}\,\boldsymbol{a}_{\boldsymbol{Lnw}} \tag{100}$$

$$\boldsymbol{A}_{\boldsymbol{b,Lnw}} = \frac{1}{2}\rho U_{yz}\begin{bmatrix} 2HC_D\,\chi_{D,a_D} & 0 & (HC'_D - BC_L)\chi_{D,a_L} \\ 0 & 0 & 0 \\ 2BC_L\,\chi_{L,a_D} & 0 & (BC'_L + HC_D)\chi_{L,a_L} \\ 0 & 0 & 0 \\ 2B^2\,C_M\,\chi_{M,a_D} & 0 & B^2C'_M\,\chi_{M,a_L} \\ 0 & 0 & 0 \end{bmatrix} \tag{101}$$

Where $\chi_{i,j}$ are the cross-sectional admittance functions associated with the aerodynamic coefficient C_i and the turbulence component j.

Alternative representations of the $\boldsymbol{A_b}$ matrix can be easily obtained by pre- and/or post-multiplication with the right transformation matrices.

Example 1. To obtain the $\boldsymbol{A}_{\boldsymbol{b,LnwGw}}$ matrix, which instead is to be post-multiplied with $\boldsymbol{a}_{\boldsymbol{Gw}}$, $\boldsymbol{A}_{\boldsymbol{b,Lnw}}$ can be simply post-multiplied by $\boldsymbol{T}_{\boldsymbol{LnwGw}}$ (eq. (102)).

$$\widetilde{\boldsymbol{f}}_{\boldsymbol{b,Lnw}} \approx \boldsymbol{A}_{\boldsymbol{b,Lnw}}\,\boldsymbol{a}_{\boldsymbol{Lnw}} = \boldsymbol{A}_{\boldsymbol{b,Lnw}}\,\boldsymbol{T}_{\boldsymbol{LnwGw}}\,\boldsymbol{T}_{\boldsymbol{GwLnw}}\,\boldsymbol{a}_{\boldsymbol{Lnw}} = \boldsymbol{A}_{\boldsymbol{b,LnwGw}}\,\boldsymbol{a}_{\boldsymbol{Gw}} \tag{102}$$

Example 2. For the same matrix to return forces in the Ls system, it can be pre-multiplied by $\boldsymbol{T}_{\boldsymbol{LsLnw}}$ (eq. (103)).

$$\widetilde{\boldsymbol{f}}_{\boldsymbol{b,Ls}} \approx \boldsymbol{A}_{\boldsymbol{b,LsGw}}\,\boldsymbol{a}_{\boldsymbol{Gw}} = \boldsymbol{T}_{\boldsymbol{LsLnw}}\boldsymbol{A}_{\boldsymbol{b,LnwGw}}\,\boldsymbol{a}_{\boldsymbol{Gw}} \tag{103}$$

4.3. Fluctuating wind forces due to turbulence and structural motions

4.3.1. Non-linear forces

Analogously to section 3.2, and using the variables defined in section 4.1, the turbulence- and motion-dependent vector of aerodynamic forces, per unit length, at each element and at each time step, represented in the Lnw system, is described by eqs. (104) and (105).

$$\widetilde{\widetilde{\boldsymbol{f}}}_{\boldsymbol{ad,Lnw}} = \boldsymbol{T}_{\boldsymbol{Lnw}\widetilde{\widetilde{\boldsymbol{Lnw}}}}\,1\big/2\,\rho\,\widetilde{\widetilde{U}}{}^2_{\widetilde{yz}}\,\boldsymbol{B}_{\boldsymbol{Lnw}}\,\widetilde{\widetilde{\boldsymbol{C}}}_{\widetilde{\widetilde{\boldsymbol{Lnw}}}} \tag{104}$$

$$\boldsymbol{T}_{\boldsymbol{Lnw}\widetilde{\widetilde{\boldsymbol{Lnw}}}} = \boldsymbol{T}_{\boldsymbol{LnwLs}}\,\boldsymbol{T}_{\boldsymbol{Ls}\widetilde{\boldsymbol{Ls}}}\,\boldsymbol{T}_{\widetilde{\boldsymbol{Ls}}\widetilde{\widetilde{\boldsymbol{Lnw}}}} \tag{105}$$

Where $\widetilde{\widetilde{\boldsymbol{C}}}_{\widetilde{\widetilde{\boldsymbol{Lnw}}}}(\widetilde{\widetilde{\theta}}_{\widetilde{yz}}) = [\widetilde{\widetilde{C}}_{\widetilde{\widetilde{D}}}, 0, \widetilde{\widetilde{C}}_{\widetilde{\widetilde{L}}}, 0, \widetilde{\widetilde{C}}_{\widetilde{\widetilde{M}}}, 0]^T$ is the vector of aerodynamic coefficients, represented in the $\widetilde{\widetilde{Lnw}}$ system and dependent on $\widetilde{\widetilde{\theta}}_{\widetilde{yz}}$.

4.3.2. Linearizations

The vector of turbulence- and motion-dependent aerodynamic forces $\widetilde{\widetilde{f}}_{ad,Lnw}$ is a non-linear function of u, v, w, Δ and $\dot{\Delta}$. The linearization process conducted in section 3.2.2 can then be repeated here.

Limitation: Analogously to the limitation described for the linear expressions in section 4.2.2, the linear approximations presented in this section should not be used whenever $\widetilde{\widetilde{U}}_{\widetilde{\widetilde{y}}}$ oscillates between positive and negative values, i.e. in the vicinity of $\beta \sim \pm 90°$, since the functions $\boldsymbol{T}_{\widetilde{\widetilde{Lnw}}Lnw}$ and $\widetilde{\widetilde{\theta}}_{\widetilde{\widetilde{yz}}}$ will have singularities at $\widetilde{\widetilde{\beta}} = \pm 90°$. It is thus assumed that $\widetilde{\widetilde{S}} = \widetilde{S} = S$ for all time steps.

Analogously to the definition of $\widetilde{\widetilde{u}}$, $\widetilde{\widetilde{v}}$ and $\widetilde{\widetilde{w}}$, when a_D, a_A and a_L account for the relative velocity between the wind and the structure, they are denoted $\widetilde{\widetilde{a}}_D$, $\widetilde{\widetilde{a}}_A$ and $\widetilde{\widetilde{a}}_L$, as in eqs. (106)–(108).

$$\widetilde{\widetilde{a}}_D = a_D - \dot{\Delta}_D \tag{106}$$

$$\widetilde{\widetilde{a}}_A = a_A - \dot{\Delta}_A \tag{107}$$

$$\widetilde{\widetilde{a}}_L = a_L - \dot{\Delta}_L \tag{108}$$

With the newly defined variables, following the same linearization principles as in section 3.2.2 and representing the structural motions in the Lnw system as $\Delta_{Lnw} = [\Delta_D, \Delta_A, \Delta_L, \Delta_{rD}, \Delta_M, \Delta_{rL}]^T = \boldsymbol{T}_{LnwLs}\Delta_{Ls}$ and $\dot{\Delta}_{Lnw} = [\dot{\Delta}_D, \dot{\Delta}_A, \dot{\Delta}_L, \dot{\Delta}_{rD}, \dot{\Delta}_M, \dot{\Delta}_{rL}]^T = \boldsymbol{T}_{LnwLs}\dot{\Delta}_{Ls}$, then $\widetilde{\widetilde{U}}_{\widetilde{\widetilde{yz}}}^2$, $\widetilde{\widetilde{\theta}}_{\widetilde{\widetilde{yz}}}$, $\boldsymbol{T}_{\widetilde{\widetilde{Lnw}}Lnw}$ and $\widetilde{\widetilde{\boldsymbol{C}}}_{\widetilde{\widetilde{Lnw}}}$ can be simplified into eqs. (109)–(112).

$$\widetilde{\widetilde{U}}_{\widetilde{\widetilde{yz}}}^{2} \approx U_{yz}\left(U_{yz} + 2\widetilde{\widetilde{a}}_D + 2SU\Delta_{rL}\sin\beta\cos\theta\right) \tag{109}$$

$$\widetilde{\widetilde{\theta}}_{\widetilde{\widetilde{yz}}} = \theta_{yz} + \widetilde{\widetilde{\Delta\theta}}_{\widetilde{\widetilde{yz}}} = \theta_{yz} + \Delta_M + \left(\widetilde{\widetilde{a}}_L - SU\Delta_{rD}\sin\beta\cos\theta\right)/U_{yz} \tag{110}$$

$$\boldsymbol{T}_{\widetilde{\widetilde{Lnw}}Lnw}(\widetilde{\widetilde{S}} = S) \approx \begin{bmatrix} 1 & -\Delta_{rL} & -\widetilde{\widetilde{\Delta\theta}}_{\widetilde{\widetilde{yz}}} + \Delta_M \\ \Delta_{rL} & 1 & -\Delta_{rD} \\ \widetilde{\widetilde{\Delta\theta}}_{\widetilde{\widetilde{yz}}} - \Delta_M & \Delta_{rD} & 1 \end{bmatrix} \tag{111}$$

$$\widetilde{\widetilde{\boldsymbol{C}}}_{\widetilde{\widetilde{Lnw}}} \approx \boldsymbol{C}_{Lnw} + \boldsymbol{C}'_{Lnw}\,\widetilde{\widetilde{\Delta\theta}}_{\widetilde{\widetilde{yz}}} \tag{112}$$

Note that $\boldsymbol{T}_{\widetilde{\widetilde{Lnw}}Lnw}$ is independent of Δ_M since such a bridge rotation leaves both the wind projection and the drag, axial and lift directions unchanged.

Finally, the vector of linearized wind forces due to the normal-projected wind and the structural motions, $\widetilde{\widetilde{f}}_{b,Lnw} = \widetilde{\widetilde{f}}_{ad,Lnw} - f_{mean,Lnw}$, can be linearized into eqs. (113)–(117).

$$[\boldsymbol{A}_{\Delta_{rD}} \quad \boldsymbol{A}_{\Delta_M} \quad \boldsymbol{A}_{\Delta_{rL}}] = \frac{1}{2}\rho U_{yz}^2 \begin{bmatrix} S\left(BC_L - HC'_D\right)\sin\beta\cos\theta\, U/U_{yz} & HC'_D & 2SHC_D\sin\beta\cos\theta\, U/U_{yz} \\ -BC_L & 0 & HC_D \\ -S\left(HC_D + BC'_L\right)\sin\beta\cos\theta\, U/U_{yz} & BC'_L & 2SBC_L\sin\beta\cos\theta\, U/U_{yz} \\ 0 & 0 & -B^2C_M \\ -SB^2C'_M\sin\beta\cos\theta\, U/U_{yz} & B^2C'_M & 2SB^2C_M\sin\beta\cos\theta\, U/U_{yz} \\ B^2C_M & 0 & 0 \end{bmatrix} \tag{115}$$

$$\widetilde{\widetilde{f}}_{b,Lnw} \approx \widetilde{f}_{b,Lnw} + \boldsymbol{A}_{\Delta,Lnw}\,\Delta_{Lnw} + \boldsymbol{A}_{\dot{\Delta},Lnw}\,\dot{\Delta}_{Lnw} \tag{113}$$

$$\boldsymbol{A}_{\Delta,Lnw} = [\boldsymbol{0} \quad \boldsymbol{0} \quad \boldsymbol{0} \quad \boldsymbol{A}_{\Delta_{rD}} \quad \boldsymbol{A}_{\Delta_M} \quad \boldsymbol{A}_{\Delta_{rL}}] \tag{114}$$

$$\boldsymbol{A}_{\dot{\Delta},Lnw} = [\boldsymbol{A}_{\dot{\Delta}_D} \quad \boldsymbol{A}_{\dot{\Delta}_A} \quad \boldsymbol{A}_{\dot{\Delta}_L} \quad \boldsymbol{0} \quad \boldsymbol{0} \quad \boldsymbol{0}] \tag{116}$$

$$[\boldsymbol{A}_{\dot{\Delta}_D} \quad \boldsymbol{A}_{\dot{\Delta}_A} \quad \boldsymbol{A}_{\dot{\Delta}_L}] = -\boldsymbol{A}_{b,Lnw}(\chi_{i,j} = 1) \tag{117}$$

Where $\widetilde{f}_{b,Lnw}$ is described and linearized in section 4.2, $\boldsymbol{0} = [0, 0, 0, 0, 0, 0]^T$ and $\boldsymbol{A}_{b,Lnw}(\chi_{i,j} = 1)$ is found in eq. (101) with all $\chi_{i,j} = 1$. Note that both Δ_{rD} and Δ_{rL} cause a change in the normal plane, from yz to $\widetilde{\widetilde{yz}}$, which consequently changes the normal projection of the wind.

4.4. Axial force contribution

4.4.1. Non-linear forces

The mean axial force $f_{mean,axial}$, the instantaneous axial force $\widetilde{f}_{ad,axial}$ and the motion-dependent instantaneous axial force $\widetilde{\widetilde{f}}_{ad,axial}$ are described in eqs. (118)–(120), for each bridge element, as vectors in the consistent Ls system.

$$f_{mean,axial,Ls} = [1/2\rho U_x|U_x|BC_x, 0, 0, 0, 0, 0]^T \tag{118}$$

$$\widetilde{f}_{ad,axial,Ls} = [1/2\rho\widetilde{U}_x|\widetilde{U}_x|BC_x, 0, 0, 0, 0, 0]^T \tag{119}$$

$$\widetilde{\widetilde{f}}_{ad,axial,Ls} = \boldsymbol{T}_{\widetilde{\widetilde{Ls}}Ls}[1/2\rho\widetilde{\widetilde{U}}_{\widetilde{\widetilde{x}}}|\widetilde{\widetilde{U}}_{\widetilde{\widetilde{x}}}|BC_x, 0, 0, 0, 0, 0]^T \tag{120}$$

In this section, $C_x = C_x(\beta = -\pi/2, \theta = 0)$ can be directly obtained for the case when the wind is parallel to the bridge girder. It is normalized by B (or alternatively by the perimeter of the cross-section), non-negative and assumed independent of both β and θ (the β-dependency of the force is already considered in U_x). This results in maximum axial forces when the wind is parallel to the longitudinal axis. However, it should be noted that the maximum axial force may occur for skew angles (see e.g. (Veritas, 2010) and their reference to (Eames, 1968) with respect to inclined cylinders). Alternatively, C_x can be obtained by curve fitting the results of different skew wind cases.

Each of the force vectors $f_{mean,axial}$, $\widetilde{f}_{ad,axial}$ and $\widetilde{\widetilde{f}}_{ad,axial}$ can be then added to their (non-axial) counterparts in sections 4.2 and 4.3, within the same coordinate system.

4.4.2. Linearizations

The linearized axial force contribution is most conveniently expressed in the Ls system (in the Lnw system, the $\widetilde{A}$ and $\widetilde{\widetilde{A}}$ axes invert in the vicinity of $\widetilde{\beta} \sim \pm 90^\circ$ and $\widetilde{\widetilde{\beta}} \sim \pm 90^\circ$).

The vector of turbulence components in the *Ls* system $\boldsymbol{a_{Ls}}$, as well as the linearized expressions for $\widetilde{U}_x|\widetilde{U}_x|$ and $\widetilde{\widetilde{U}}_{\underset{\sim}{x}}|\widetilde{\widetilde{U}}_{\underset{\sim}{x}}|$ are introduced in eqs. (121)–(123).

$$\boldsymbol{a_{Ls}} = [a_x, a_y, a_z]^T = \left[\widetilde{U}_x - U_x, \widetilde{U}_y - U_y, \widetilde{U}_z - U_z\right]^T = \boldsymbol{T_{LsGw}}[u, v, w]^T \tag{121}$$

$$\widetilde{U}_x|\widetilde{U}_x| \approx U_x|U_x| + 2|U_x|a_x \tag{122}$$

$$\widetilde{\widetilde{U}}_{\underset{\sim}{x}}|\widetilde{\widetilde{U}}_{\underset{\sim}{x}}| \approx U_x|U_x| + 2|U_x|\left((a_x - \dot{\Delta}_x) + U_y\Delta_{rz} - U_z\Delta_{ry}\right) \tag{123}$$

Then, the linear approximations of $\widetilde{\boldsymbol{f}}_{\boldsymbol{ad,axial,Ls}}$ and $\widetilde{\widetilde{\boldsymbol{f}}}_{\boldsymbol{ad,axial,Ls}}$ are expressed in eqs. (124)–(130).

$$\widetilde{\boldsymbol{f}}_{\boldsymbol{ad,axial,Ls}} \approx \boldsymbol{f_{mean,axial,Ls}} + \boldsymbol{A_{b,axial,Ls}}\,\boldsymbol{a_{Ls}} \tag{124}$$

$$\widetilde{\widetilde{\boldsymbol{f}}}_{\boldsymbol{ad,axial,Ls}} \approx \widetilde{\boldsymbol{f}}_{\boldsymbol{ad,axial,Ls}} + \boldsymbol{A_{\Delta,axial,Ls}}\boldsymbol{\Delta_{Ls}} + \boldsymbol{A_{\dot{\Delta},axial,Ls}}\boldsymbol{\dot{\Delta}_{Ls}} \tag{125}$$

$$\boldsymbol{A_{b,axial,Ls}} = 1 \Big/ 2\rho B|U_x| \begin{bmatrix} 2C_x\chi_{x,a_x} & 0 & 0 \\ 0 & 0 & 0 \\ 0 & 0 & 0 \\ 0 & 0 & 0 \\ 0 & 0 & 0 \\ 0 & 0 & 0 \end{bmatrix} \tag{126}$$

$$\boldsymbol{A_{\Delta,axial,Ls}} = \begin{bmatrix} \boldsymbol{0} & \boldsymbol{0} & \boldsymbol{0} & \boldsymbol{A_{\Delta_{rx}}} & \boldsymbol{A_{\Delta_{ry}}} & \boldsymbol{A_{\Delta_{rz}}} \end{bmatrix}_{axial} \tag{127}$$

$$\begin{bmatrix} \boldsymbol{A_{\Delta_{rx}}} & \boldsymbol{A_{\Delta_{ry}}} & \boldsymbol{A_{\Delta_{rz}}} \end{bmatrix}_{axial} = 1 \Big/ 2\rho B|U_x| \begin{bmatrix} 0 & -2U_zC_x & 2U_yC_x \\ 0 & 0 & U_xC_x \\ 0 & -U_xC_x & 0 \\ 0 & 0 & 0 \\ 0 & 0 & 0 \\ 0 & 0 & 0 \end{bmatrix} \tag{128}$$

$$\boldsymbol{A_{\dot{\Delta},axial,Ls}} = \begin{bmatrix} \boldsymbol{A_{\dot{\Delta}_x}} & \boldsymbol{A_{\dot{\Delta}_y}} & \boldsymbol{A_{\dot{\Delta}_z}} & \boldsymbol{0} & \boldsymbol{0} & \boldsymbol{0} \end{bmatrix}_{axial} \tag{129}$$

$$\begin{bmatrix} \boldsymbol{A_{\dot{\Delta}_x}} & \boldsymbol{A_{\dot{\Delta}_y}} & \boldsymbol{A_{\dot{\Delta}_z}} \end{bmatrix}_{axial} = -\boldsymbol{A_{b,axial,Ls}}\left(\chi_{x,a_x} = 1\right) \tag{130}$$

Where $\boldsymbol{0} = [0,0,0,0,0,0]^T$ and where χ_{x,a_x} is the cross-sectional admittance function associated with the aerodynamic coefficient C_x and the $\boldsymbol{x}$-projected turbulence a_x.

5. Response analysis

5.1. Time domain approach

In the time-domain, the equation of motion for a dynamic structural system under forced vibration is expressed by eq. (131), with the global buffeting forces on the right-hand side.

$$\boldsymbol{M^G}\ddot{\Delta}^G(t) + \boldsymbol{C^G}\dot{\Delta}^G(t) + \boldsymbol{K^G}\Delta^G(t) = \boldsymbol{F_b^G}(t) \tag{131}$$

Here $\boldsymbol{M^G}$, $\boldsymbol{C^G}$ and $\boldsymbol{K^G}$ are the global mass, damping and stiffness matrices, with size $[6N_N \times 6N_N]$, with N_N as the number of structural nodes in a FEM model, where each node has 6 DOF; Δ^G, $\dot{\Delta}^G$ and $\ddot{\Delta}^G$ are the global vectors of structural displacements, velocities, and accelerations, with size $[6N_N]$; $\boldsymbol{F_b^G}$ is the global vector of nodal buffeting forces, with size $[6N_N]$, assembled from all the elemental $\widetilde{\boldsymbol{F}}_{\boldsymbol{b}} = L\widetilde{\boldsymbol{f}}_{\boldsymbol{b}}$ or $\widetilde{\widetilde{\boldsymbol{F}}}_{\boldsymbol{b}} = L\widetilde{\widetilde{\boldsymbol{f}}}_{\boldsymbol{b}}$ vectors. These global matrices and vectors are assembled following standard FEM techniques and are represented in a global and consistent coordinate system such as the *Gs* system.

To numerically simulate the turbulent wind field, the turbulence simulator *TurbSim* (Jonkman, 2009) or the freely available *MATLAB* code by Etienne Cheynet (2020) can be used.

To solve the equation of motion, a numerical integration method such as the Newmark-beta method (Newmark, 1959), can be used.

In a linearized format, the motion-dependent force coefficient matrices $\boldsymbol{A_\Delta}$ and $\boldsymbol{A_{\dot{\Delta}}}$ can be moved to the left-hand side of the equation of motion, joining the other Δ and $\dot{\Delta}$ dependencies, instead of contributing to the global vector $\boldsymbol{F_b^G}$. Thus, they can be converted into the so-called aerodynamic stiffness $\boldsymbol{K_{AE}^G}$ and aerodynamic damping $\boldsymbol{C_{AE}^G}$ global matrices. $\boldsymbol{K_{AE}^G}$ and $\boldsymbol{C_{AE}^G}$ are expressed in the *Gs* system so that they can be added to the structural stiffness $\boldsymbol{K_S^G}$ and structural damping $\boldsymbol{C_S^G}$ global matrices, as in eqs. (132) and (133).

$$\boldsymbol{K^G} = \boldsymbol{K_S^G} + \boldsymbol{K_{AE}^G} \tag{132}$$

$$\boldsymbol{C^G} = \boldsymbol{C_S^G} + \boldsymbol{C_{AE}^G} \tag{133}$$

They have the size $[6N_N \times 6N_N]$ and can be assembled from the individual $\boldsymbol{K_{AE}}$ and $\boldsymbol{C_{AE}}$ matrices representative of each element, with size $[6 \times 6]$. $\boldsymbol{K_{AE}}$ and $\boldsymbol{C_{AE}}$ are obtained through eqs. (134) and (135).

$$\boldsymbol{K_{AE}} = -\,L\,\boldsymbol{T_{GsGw}}\boldsymbol{A_{\Delta,Gw}}\boldsymbol{T_{GwGs}} \tag{134}$$

$$\boldsymbol{C_{AE}} = -\,L\,\boldsymbol{T_{GsGw}}\boldsymbol{A_{\dot{\Delta},Gw}}\boldsymbol{T_{GwGs}} \tag{135}$$

$\boldsymbol{K_{AE}}$ and $\boldsymbol{C_{AE}}$ can also be estimated in a frequency-dependent format. To express such frequency-dependent forces in the time domain, as well as the frequency-dependent cross-sectional admittance functions $\chi_{i,j}$, one approach is given in e.g. Chapter 4.7 in (Xu, 2013). In a frequency domain analysis, $\boldsymbol{K_{AE}}$ and $\boldsymbol{C_{AE}}$ can be transformed to modal coordinates and added to the modal stiffness and damping matrices, inside the modal frequency response function.

5.2. Frequency domain approach

The frequency domain approach is a Fourier transform of its time domain counterpart. In the time domain a displacement vector Δ is estimated, whereas in the frequency domain a cross spectral density matrix of the displacement response $\boldsymbol{S_{\Delta\Delta}}(\omega)$ is estimated. From known modal analyses and buffeting theory solution schemes (see e.g. (Chopra, 1995; Clough and Penzien, 2003; Strømmen, 2010; Xu, 2013)) it follows that eqs. (136)–(141) can be used to obtain the standard deviation of the displacement response $\boldsymbol{\sigma_\Delta}$. The response is here given for the *Gs* system, as a function of $\boldsymbol{S_{aa}}(\omega)$ which is naturally expressed in the *Gw* system. Single-sided spectra are used. The superscript ^{G} is omitted when there is no ambiguity.

$$\boldsymbol{\sigma_\Delta} = \sqrt{\int_0^\infty \boldsymbol{S_\Delta}(\omega)\,d\omega} \tag{136}$$

$$\boldsymbol{S_{\Delta\Delta}}(\omega) = \boldsymbol{\Phi}\,\boldsymbol{S_{\widetilde{\eta\eta}}}(\omega)\,\boldsymbol{\Phi}^T \tag{137}$$

$$\boldsymbol{S_{\widetilde{\eta\eta}}}(\omega) = \widehat{\boldsymbol{H}}^*(\omega)\,\boldsymbol{S_{\widetilde{FF}}}(\omega)\,\widehat{\boldsymbol{H}}^T(\omega) \tag{138}$$

$$\boldsymbol{S_{\widetilde{FF}}}(\omega) = \boldsymbol{\Phi}^T\,\boldsymbol{P_b^G}^*\,\boldsymbol{S_{aa}}(\omega)\,\boldsymbol{P_b^G}^T\,\boldsymbol{\Phi} \tag{139}$$

$$\widehat{\boldsymbol{H}}(\omega) = \left[-\omega^2\widehat{\boldsymbol{M}} + i\omega\widehat{\boldsymbol{C}} + \widehat{\boldsymbol{K}}\right]^{-1} \tag{140}$$

$$\boldsymbol{P_b} = L\,\boldsymbol{A_{b,GsGw}} = L\,\boldsymbol{T_{GsGw}}\boldsymbol{A_{b,Gw}} \tag{141}$$

Here $\boldsymbol{\sigma_\Delta}$ is the standard deviation of the response with size $[6N_N]$, with N_N as the number of nodes. $\boldsymbol{S_\Delta}(\omega)$ is the auto-spectral density vector of the nodal displacement response. It can be extracted from the diagonal elements of $\boldsymbol{S_{\Delta\Delta}}(\omega)$ and has size $[6N_N]$. ω is the angular frequency. $\boldsymbol{S_{\Delta\Delta}}(\omega)$ is the cross spectral density matrix of the nodal displacement response, with size $[6N_N \times 6N_N]$. $\boldsymbol{\Phi}$ is the matrix of mode shapes with size $[6N_N \times N_M]$, with N_M as the number of modes. $\boldsymbol{S}_{\widehat{\eta\eta}}(\omega)$ is the cross-spectral density matrix of the modal displacement response with size $[N_M \times N_M]$. $\widehat{\boldsymbol{H}}(\omega)$ is the modal frequency response function matrix with size $[N_M \times N_M]$. In the absence of modal-coupling it becomes a diagonal matrix. $\boldsymbol{S}_{\widehat{FF}}(\omega)$ is the cross-spectral density matrix of the modal buffeting loads with size $[N_M \times N_M]$. $\boldsymbol{S}_{aa}(\omega)$ is the cross-spectral density matrix of the turbulence components u, v and w, with size $[3N_N \times 3N_N]$. One possible formulation of $\boldsymbol{S}_{aa}(\omega)$ can be found in (Zhu and Xu, 2005). $\boldsymbol{P}_b^G$ is the global coefficient matrix of buffeting forces assembled from each elemental $\boldsymbol{P}_b$, and it has size $[6N_N \times 3N_N]$. $\boldsymbol{P}_b$ is the coefficient matrix of buffeting forces, representative of one element, with size $[6 \times 3]$. It can be frequency-dependent when the cross-sectional admittance functions $\chi_{i,j}$ are included. $\widehat{\boldsymbol{M}}$ is the modal mass matrix. It can be frequency-dependent, e.g. due to hydrodynamic forces, and it has size $[N_M \times N_M]$. $\widehat{\boldsymbol{C}}$ and $\widehat{\boldsymbol{K}}$ are the modal damping and modal stiffness matrices. They can also be frequency-dependent and have size $[N_M \times N_M]$ each. *(superscript) represents the complex conjugate. i is the imaginary unit.

To express the response in the Ls system instead, for each element, the $\boldsymbol{S}_{\Delta\Delta}(\omega)$ in eq. (137) can be converted to an elemental format, and then pre- and post-multiplied by $\boldsymbol{T}_{LsGs}$ and $\boldsymbol{T}_{GsLs}$, accordingly.

6. Conclusions

Previous literature, through experimental and field measurements, has revealed an important impact of skew winds on the response of bridges. Two theoretical models to estimate the skew wind buffeting loads, here named 3D and 2D, are found in the literature. The 3D approach, which requires aerodynamic coefficients that depend on both yaw and inclination angles, is preferred, but not always feasible. The 2D approach, where only the normal projection of the wind is considered, has previously underestimated the buffeting response of straight bridges to some extent, raising further questions for bridges with more complex geometries.

A revised version of the bridge buffeting theory for skew winds is introduced here, for both turbulence- and motion-dependent forces. The 3D approach presented consists of a partial revision and a complement to the comprehensive and pioneering work by Le-Dong Zhu. Through the use of convenient coordinate systems, an intuitive and systematic use of transformation matrices, and with the help of modern mathematical tools, a few key improvements were achieved for the 3D approach:

1. A simplified and accurate description of the wind velocities, yaw angles, inclination angles and transformation matrices, as functions of both the turbulence and the structural motions;
2. A clear and compact representation of the linearized buffeting forces;
3. A more accurate description of the quasi-static motion-dependent forces, in both non-linear and linear forms.

Additionally, for the cases where the 3D approach is not feasible and in order to establish a better framework of comparison, a comprehensive 2D approach is developed:

1. The *cosine rule* is expanded to include wind directions that are both yawed and inclined;
2. An optional axial force contribution, when the axial coefficient has been estimated, is included, accounting for both turbulence- and motion-dependent forces;
3. The motion-dependencies are expanded, from the typical 3 DOF in the normal plane to a complete 6 DOF formulation;
4. Linearizations of all relevant forces and variables are successfully achieved and presented in a conveniently compact form.

Further work is necessary to evaluate the impact of skew winds on bridges with different geometries, to compare the differences between the two approaches and to evaluate the improvements and generalizations introduced here. A separate article addressing some of these aspects is expected to follow the present work, where the planned bridge for Bjørnafjorden will be used as a case study.

CRediT authorship contribution statement

Bernardo Morais da Costa: Conceptualization, Methodology, Software, Validation, Formal analysis, Investigation, Writing – original draft, Writing – review & editing, Visualization, Project administration, Funding acquisition. **Jungao Wang:** Conceptualization, Software, Validation, Writing – review & editing, Supervision, Project administration, Funding acquisition. **Jasna Bogunović Jakobsen:** Conceptualization, Validation, Writing – review & editing, Supervision, Project administration, Funding acquisition. **Ole Andre Øiseth:** Conceptualization, Writing – review & editing. **Jónas Þór Snæbjörnsson:** Conceptualization, Writing – review & editing.

Declaration of competing interest

The authors declare that they have no known competing financial interests or personal relationships that could have appeared to influence the work reported in this paper.

Acknowledgements

The authors gratefully acknowledge the Norwegian Public Roads Administration (Norway), for the general research support within the innovative E39 Coastal Highway Route project, as well as The Research Council of Norway (Norway).

Appendix. Key differences between the original and the present theory

Original theory (Zhu, 2002)	The present theory
Local static structural coordinate systems:	
Use of both a Ls $(\boldsymbol{x},\boldsymbol{y},\boldsymbol{z})$ and a Lr $(\boldsymbol{q},\boldsymbol{p},\boldsymbol{h})$ system for each element. The direction of the $\boldsymbol{p}$-axis is dependent on the mean wind such that $\overline{\beta} \leq 90°$.	Use of only one Ls $(\boldsymbol{x},\boldsymbol{y},\boldsymbol{z})$ system that is consistent regardless of mean wind direction, i.e. for $\beta \in]-180°,180°]$. This consistency leads to simpler expressions.
Mean wind coordinate systems:	
Use of both a local $L\overline{w}$ $(\overline{\boldsymbol{q}},\overline{\boldsymbol{p}},\overline{\boldsymbol{h}})$ system and a global Gw $(\boldsymbol{X}_u,\boldsymbol{Y}_v,\boldsymbol{Z}_w)$ system to represent the mean wind.	The $L\overline{w}$ $(\overline{\boldsymbol{q}},\overline{\boldsymbol{p}},\overline{\boldsymbol{h}})$ system is discarded (redundant) and only Gw $(\boldsymbol{X}_u,\boldsymbol{Y}_v,\boldsymbol{Z}_w)$ is used for the mean wind.
Local dynamic structural coordinate systems:	
Not included. Element rotations and their effects on motion dependent forces must be explicitly defined.	Inclusion of a $\widetilde{\widetilde{Ls}}$ $(\widetilde{\widetilde{\boldsymbol{x}}},\widetilde{\widetilde{\boldsymbol{y}}},\widetilde{\widetilde{\boldsymbol{z}}})$ system, solidary with the moving element, helping define the motion dependent loads.

(*continued on next page*)

(*continued*)

Original theory (Zhu, 2002)	The present theory
Instantaneous and relative wind coordinate systems:	
The $\widetilde{\boldsymbol{p}}$ in the $L\widetilde{w}$ $(\widetilde{\boldsymbol{q}}, \widetilde{\boldsymbol{p}}, \widetilde{\boldsymbol{h}})$ system follows the instantaneous wind. No system is dedicated to the instantaneous relative wind (relative to the bridge in motion).	The $\boldsymbol{X}_{\widetilde{U}}$ in the $\widetilde{Lw}(\boldsymbol{X}_{\widetilde{U}}, \boldsymbol{Y}_{\widetilde{U}}, \boldsymbol{Z}_{\widetilde{U}})$ system is aligned with the instantaneous wind $(\widetilde{U})$. The $\boldsymbol{X}_{\widetilde{\widetilde{U}}}$ in the $\widetilde{\widetilde{Lw}}(\boldsymbol{X}_{\widetilde{\widetilde{U}}}, \boldsymbol{Y}_{\widetilde{\widetilde{U}}}, \boldsymbol{Z}_{\widetilde{\widetilde{U}}})$ system is aligned with the relative instantaneous wind $(\widetilde{\widetilde{U}})$.
Transformation matrices:	
Transformation matrices are deduced from 9 angles between the axes of both systems, which must be previously defined.	An intuitive formulation using chained rotations is also included.
Linearization of the aerodynamic loads:	
$\overline{\boldsymbol{A}}^b$, $\Delta\beta$, $\Delta\theta$, $\boldsymbol{T}_{L\overline{w}L\widetilde{w}}$ are formulated as functions of U, v, w, the nine entries t_{ij} of the transformation matrix $\boldsymbol{T}_{LrGw}$ and six expressions s_i of these. $\overline{\boldsymbol{A}}^b$ "transforms" $\boldsymbol{a} = [u, v, w]^T$ from the Gw system into forces in the $L\overline{w}$ system.	$\boldsymbol{A}_b$, $\widetilde{\Delta\beta}$, $\widetilde{\Delta\theta}$, $\boldsymbol{T}_{Gw\widetilde{Lw}}$ are clearly formulated as functions of only U, u, v, w, β and θ, in a compact form and without loss of generality. $\boldsymbol{A}_b$ and $\boldsymbol{a} = [u, v, w]^T$ are both represented in the Gw system.
Motion-dependent forces:	
It is implicitly assumed (see section 5.4.3 in (Zhu, 2002), in particular eq. (5.12b)) that: $\widetilde{\widetilde{\beta}} \approx \beta + \frac{v}{U\cos\theta} - \Delta_{rz}$ $\widetilde{\widetilde{\theta}} \approx \theta + \frac{w}{U} + \Delta_{rY_v}$ The quasi-static expressions of P_3^*, H_3^* and A_3^* in eq. 5-16 are inaccurate: there is an inaccuracy in $\widetilde{\widetilde{\beta}}$ with respect to the bridge rotation ($\Delta_{rz} \neq \frac{\Delta_{rZ_w}}{\cos\theta}$, for $\theta \neq 0$), and a motion dependent $\boldsymbol{T}_{L\overline{w}L\widetilde{w}}$ (analogous to $\boldsymbol{T}_{Gw\widetilde{\widetilde{Lw}}}$) is missing in the second term of the right side of eq. 5-13. Some motion dependencies are thus overlooked. After eq. 5-13, it is mentioned that $\overline{\boldsymbol{A}}^{se} = \overline{\boldsymbol{A}}^b(\chi_{i,j} = 1)$, where the relevant $\boldsymbol{T}_{L\overline{w}L\widetilde{w}}$ effects have been included. This confines the inaccuracies to the aerodynamic stiffness only, not the aerodynamic damping. A typo in P_5^* in eq. 5–16: $[\sin\overline{\beta}\cos\overline{\beta}]C'^{\theta}_{C_{\overline{q}}}$ should be corrected to $[\sin\overline{\beta}\cos\overline{\theta}]C'^{\theta}_{C_{\overline{q}}}$.	A simple non-linear quasi-static description of motion dependent forces is first provided in eq. (52). Linear approximations of $\widetilde{\widetilde{\beta}}$ and $\widetilde{\widetilde{\theta}}$ are derived and revised to: $\widetilde{\widetilde{\beta}} \approx \beta + \frac{v - \dot{\Delta}_{Y_v}}{U\cos\theta} - \frac{\Delta_{rZ_w}}{\cos\theta}$ $\widetilde{\widetilde{\theta}} \approx \theta + \frac{w - \dot{\Delta}_{Z_w}}{U} + \Delta_{rY_v}$ A $\boldsymbol{T}_{Gw\widetilde{\widetilde{Lw}}}$ is derived and used, and a linear approximation is also provided. Comprehensive formulations of $\boldsymbol{A}_{\Delta}$ and $\boldsymbol{A}_{\dot{\Delta}}$ are provided. Accurate quasi-static Scanlan's flutter derivatives are provided as an alternative.
Alternative approach when the estimation of $\boldsymbol{C}(\beta, \theta)$ is unfeasible and only $\boldsymbol{C}(0, \theta)$ are known:	
A cosine rule $\boldsymbol{C}_{Ls}(\beta,\theta) = \boldsymbol{C}_{Ls}(0,\theta)\cos^2\beta$, originally intended for $\theta = 0$, is used to compare equivalent aerodynamic coefficients for different β (0 to 35°) and θ (− 10 to 10°) (see also (Zhu et al., 2002b)). $C_{D_p}(= C_y)$ show moderate deviations. $C_{L_h}(= C_z)$ show erratic deviations. $C_{M_\alpha}(= C_{rx})$ show large deviations, especially for $\theta = \pm 10°$.	A novel generalization of the cosine rule approach is introduced, for generic values of both β and θ, allowing for contributions from axial forces and motion-dependent forces, due to in- and out-of-plane motions. All the relevant variables, deductions and linearizations are presented. This novel approach is still only intended for preliminary analyses and comparison purposes, as it is presumably inferior to the 3D $\boldsymbol{C}(\beta, \theta)$ approach.

References

Bathe, K.-J., 2006. Finite Element Procedures. Klaus-Jurgen Bathe.

Bursnall, W.J., Loftin Jr., L.K., 1951. Experimental Investigation of the Pressure Distribution about a Yawed Circular Cylinder in the Critical Reynolds Number Range. National Aeronautics and Space Administration, Washington DC.

Cheynet, E., 2020. Wind Field Simulation (Text-based Input). Zenodo. Retrieved from. https://zenodo.org/record/3823864.

Chopra, A.K., 1995. Dynamics of Structures, a Primer. Earthquake Engineering Research.

Clough, R.W., Penzien, J., 2003. Dynamics of Structures. Computers and Structures, Berkeley. CA.

Davenport, A.G., 1961. The application of statistical concepts to the wind loading of structures. Proc. Inst. Civ. Eng. 19, 449–472.

Eames, M.C., 1968. Steady-state theory of towing cables. Trans. RINA 110, 185–206.

Ersdal, S., Faltinsen, O.M., 2006. Normal forces on cylinders in near-axial flow. J. Fluid Struct. 22, 1057–1077.

Huang, M.-H., Lin, Y.-Y., Weng, M.-X., 2012. Flutter and buffeting analysis of bridges subjected to skew wind. J. Appl. Sci. Eng. 15, 401–413.

Hutton, D.V., 2004. Fundamentals of Finite Element Analysis. McGraw-hill.

Jian, B., Su, Y., Li, M., 2020. Buffeting response of cable-stayed bridge during construction under skew winds and pylon interference. KSCE J. Civil Eng. 24, 2971–2979.

Jones, R.T., 1947. Effects of Sweepback on Boundary Layer and Separation.

Jonkman, B.J., 2009. TurbSim User's Guide: Version 1.50. National Renewable Energy Lab.(NREL), Golden, CO (United States).

Kimura, K., Tanaka, H., 1992. Bridge buffeting due to wind with yaw angles. J. Wind Eng. Ind. Aerod. 42, 1309–1320.

Li, S., Li, M., Zhang, L., 2016. Buffeting response of cable-stayed bridge under skew wind. In: Proceedings of the Advances in Civil. Environmental and Materials Research.

Newmark, N.M., 1959. A method of computation for structural dynamics. J. Eng. Mech. Div. 85, 67–94.

Relf, E., Powell, C., 1917. Tests on smooth and stranded wires inclined to the wind direction and a comparison of the results on stranded wires in air and water. Advisory Committe for Aeronautics. Reports and Memoranda (New Series) 307, 8–14.

Scanlan, R.H., 1993. Bridge buffeting by skew winds in erection stages. J. Eng. Mech. 119, 251–269.

Scanlan, R.H., Tomo, J., 1971. Air Foil and Bridge Deck Flutter Derivatives. Journal of Soil Mechanics & Foundations Div.

Sears, W.R., 1948. The boundary layer of yawed cylinders. J. Aeronaut. Sci. 15, 49–52.

Strømmen, E., 2010. Theory of Bridge Aerodynamics. Springer Science & Business Media.

Sumer, B.M., 2006. Hydrodynamics Around Cylindrical Strucures. World scientific.

Tanaka, H., Davenport, A.G., 1982. Response of taut strip models to turbulent wind. J. Eng. Mech. Div. 108, 33–49.

Van Atta, C., 1968. Experiments on vortex shedding from yawed circular cylinders. AIAA J. 6, 931–933.

Veritas, D.N., 2010. Recommended Practice DNV-RP-C205: Environmental Conditions and Environmental Loads. DNV, Norway.

Wang, H., Li, A.Q., Hu, R.M., 2011. Comparison of ambient vibration response of the Runyang suspension bridge under skew winds with time-domain numerical predictions. J. Bridge Eng. 16, 513–526.

Wang, R., Cheng, S.H., Ting, D.S.K., 2019. Effect of yaw angle on flow structure and cross-flow force around a circular cylinder. Phys. Fluids 31.

Wild, J.M., 1949. The boundary layer of yawed infinite wings. J. Aeronaut. Sci. 16, 41–45.

Xie, J., Tanaka, H., Wardlaw, R.L., Savage, M.G., 1991. Buffeting analysis of long span bridges to turbulent wind with yaw angle. J. Wind Eng. Ind. Aerod. 37, 65–77.

Xu, Y.-L., 2013. Wind Effects on Cable-Supported Bridges. John Wiley & Sons.

Xu, Y.L., Zhu, L.D., 2005. Buffeting response of long-span cable-supported bridges under skew winds. Part 2: case study. J. Sound Vib. 281, 675–697.

Zhu, L.-D., 2002. Buffeting Response of Long Span Cable-Supported Bridges under Skew Winds: Field Measurement and Analysis. Department of Civil and Structural Engineering. Pao Yue-kong Library, The Hong Kong Polytechnic University, Hong Kong. https://theses.lib.polyu.edu.hk/handle/200/569.

Zhu, L., Xu, Y., Xiang, H., 2002a. Tsing Ma bridge deck under skew winds—Part II: flutter derivatives. J. Wind Eng. Ind. Aerod. 90, 807–837.

Zhu, L., Xu, Y., Zhang, F., Xiang, H., 2002b. Tsing Ma bridge deck under skew winds—Part I: aerodynamic coefficients. J. Wind Eng. Ind. Aerod. 90, 781–805.

Zhu, L.D., Xu, Y.L., 2005. Buffeting response of long-span cable-supported bridges under skew winds. Part 1: Theory. J. Sound Vib. 281, 647–673.